UNIVERSITÀ DEGLI STUDI
DI MILANO

DOTTORATO DI MEDICINA MOLECOLARE E TRASLAZIONALE

CICLO XXXIII

Anno Accademico 2019/2020

TESI DI DOTTORATO DI RICERCA

MED26

INVESTIGATION OF C9ORF72 MOLECULAR HALLMARKS AND DEVELOPMENT OF THERAPEUTIC STRATEGIES

Dottorando: Fabio BIELLA

Matricola N°: R12051

TUTORE: Prof.ssa Stefania Paola CORTI

CO-TUTORE: Dott.ssa Michela TAIANA

COORDINATORE DEL DOTTORATO: Prof. Michele SAMAJA

II

SOMMARIO.

La maggior parte dei casi di Sclerosi Laterale Amiotrofica (SLA) geneticamente determinata è attribuibile all'espansione patologica nel numero di ripetizioni esanucleotidiche in una regione non codificante del locus *C9orf72*. Molti meccanismi patologici sono stati proposti per la SLA con mutazione *C9orf72*, sia la perdita di funzione che l'acquisto di funzione, quest'ultima associata alla tossicità dei foci di RNA e dell'accumulo dei dipeptidi ripetuti (DPR).
La ricerca su questo tipo di SLA è limitata dalla mancanza di modelli soddisfacenti e dal difficile accesso al tipo cellulare colpito dalla malattia. I modelli animali non sono in grado di riprodurre tutte le caratteristiche patologiche e la situazione è complicata ulteriormente dalla presenza di molti geni modificatori della malattia.

Per risolvere tali difficolta, questo studio si avvantaggia della tecnologia delle cellule staminali pluripotenti indotte (iPSC) per investigare sia le caratteristiche patologiche canoniche che non canoniche della SLA *C9orf72*. Le iPSC possiedono lo stesso background genetico degli individui affetti da cui derivano e possono essere differenziate in motoneuroni (MN) per studiarne le specifiche alterazioni; inoltre comparando le linee *C9orf72* con le loro controparti isogeniche l'influenza dei geni modificatori di malattia può essere eliminata.

Abbiamo analizzato l'accumulo di foci di RNA e DPR, segni canonici della mutazione *C9orf72,* e li abbiamo trovati aumentati nelle cellule

C9orf72 in entrambi i tipi di linee. È stato osservato anche l'incremento di danno al DNA, caratteristica patologica di più recente scoperta.

Inoltre nei MN derivati da iPSC l'espressione dei geni *SEPT7*, *STMN1* e *STMN2*, regolatori citoscheletrici con importanti funzioni neuronali, è risultata alterata nel background genetico *C9orf72* espanso.

Utilizzando i modelli in uso, abbiamo potuto valutare l'efficacia di una terapia con oligonucleotidi antisenso (ASO) basati sulla chimica morfolino (MO) come prova della fattibilità dello screening di farmaci ed in entrambi i modelli i nostri MO si sono dimostrati in grado di revertire l'accumulo di DPR e l'induzione del danno al DNA.

Inoltre abbiamo effettuato un'analisi dell'espressione genica globale. Da questo studio è emersa un'alterazione in geni coinvolti nella funzionalità neuronale nelle iPSC *C9orf72*, mentre i MN *C9orf72* mostravano una deregolazione nelle vie di segnale coinvolte nell'infiammazione e nella comunicazione cellulare, suggerendo la presenza di meccanismi patologici che non coinvolgano i soli MN. Il trattamento con i MO si è dimostrato capace di revertire queste alterazioni.

Abbiamo inoltre intrapreso la caratterizzazione di un modello di SLA-*C9orf72* basto su organoidi, un modello 3D in grado di riprodurre in modo più fisiologico la reale struttura del sistema nervoso centrale. Infatti, oltre all'accumulo di DPR, abbiamo osservato negli organoidi *C9orf72* alterazioni patologiche non riproducibili nei modelli 2D, suggerendone l'utilità come modello di malattia.

ABSTRACT.

The majority of genetic Amyotrophic Lateral Sclerosis (ALS) cases are due to the expansion in the number of an hexanucleotidic repeat in a non-coding site of the locus *C9orf72*. Many mechanisms for the *C9orf72*-ALS are suggested, both loss of function and gain of function due to RNA foci and Dipeptide Repeats (DPR) toxicity.
Research on *C9orf72*-ALS is hindered by the lack of satisfactory models and by the difficult access to the target cell type. Animal models fail to recreate all the pathological features and the situation is further complicated by the presence of many disease modifying genes.

To overcome these issues, this study takes advantages of the induced Pluripotent Stem Cells (iPSCs) technology to investigate canonical as well as more recent *C9orf72* molecular hallmarks. The iPSCs carry the same genetic background of patients and can be further differentiated in motoneurons (MNs) to study neuronal specific alteration and comparing *C9orf72*-expanded cell lines with their isogenic corrected counterpart, the influence of disease-modifying genes can be eliminated.

We analysed canonical RNA foci and DPR accumulation finding them increased in *C9orf72* samples in both models. DNA damage accumulation, a recently discovered *C9orf72*-ALS feature, was also increased.

Moreover, in iPSC-derived MNs expression of *SEPT7*, *STMN1* and *STMN2* genes, cytoskeletal regulators with important function in neuronal cells, has been found altered in *C9orf72* background.

Taking advantage of these established models we could also evaluate the efficacy of a morpholine (MO)-based antisense oligonucleotide (ASO) therapy as a proof of principle for the feasibility of drug screening in these models. We found that both our MO oligomers were able to rescue DPR accumulation and DNA damage induction.

Global gene expression analysis has also been performed. From this investigation a subtle alteration in genes related with neuronal function in iPSC was detected, while *C9orf72* MNs showed deregulation in pathways related to inflammation and cell-to-cell communication suggesting a non-cell-autonomous mechanism for the disease. Interestingly, MOs treatment could rescue these alterations.

Moving forward we started the characterization of a 3D organoid-based model of *C9orf72*-ALS that can reproduce the complexity of central nervous system. We found in organoids DPR accumulation and other disease hallmarks which could not be detected in 2D models, supporting the promising role of this 3D model.

TABLE OF CONTENTS.

RESEARCH INTEGRITY STATEMENT.

Results reported in this work comply with the four fundamental principles of research integrity of The European Code of Conduct for Research Integrity (ALLEA, Berlin, 2018):

- Reliability in ensuring the quality of research, reflected in the design, the methodology, the analysis and the use of resources;
- Honesty in developing, undertaking, reviewing, reporting and communicating research in a transparent, fair, full and unbiased way;
- Respect for colleagues, research participants, society, ecosystems, cultural heritage and the environment;
- Accountability for the research from idea to publication, for its management and organization, for training, supervision and mentoring, and for its wider impacts.

The thesis work has been evaluated by three independent referees.

- Bossolasco Patrizia, PhD
  Istituto Auxologico Italiano IRCCS, Milan, Italy
  Department of Neurology, Laboratory of Neuroscience

- Diane B. Re, PhD
  Columbia University, New York, United States
  Department of Environmental Health Science

- Rideout Hardy, PhD
  BRFAA, Athens, Greece
  Center for Clinical, Experimental Surgery and Translational Research

1. INTRODUCTION.

1.1. Amyotrophic Lateral Sclerosis (ALS).

Amyotrophic Lateral Sclerosis (ALS) is a fatal progressive neurodegenerative disease. It is the most common adult onset form of motor neurons disease, appearing often in the fifth or sixth decade of life with a mean survival after the onset of the symptoms of 3 to 5 years [1]. ALS can exist in two forms which are named familial or sporadic based on the presence of an affected individual among the close relative or not. This disease causes the degeneration of both the glutamatergic upper motor neurons (UMNs), situated in the brainstem and in the motor cortex, and the cholinergic lower motor neurons (LMNs) embedded within the ventral horn of the spinal cord.

The degeneration appears as a progressive muscle weakness and atrophy due to the loss of the targeted neurons defining its first type of classification as bulbar or spinal onset, depending on which is the first MN to degenerate [2]. For the spinal onset the LMNs are the first to be lost so, mostly, this type is characterized by loss of motor skills in the limb often on one side before the other, while the bulbar onset shows impairment of speech, swallowing and cognitive impairment. The last neurons to degenerate are the phrenic and oculomotor ones [3], they show a different kind of resistance to the pathology and often death occurs due to respiratory failure.

The only approved treatments available at the moment are Riluzole and Edaravone, they are not able to stop the disease but extend the life of the patients by only few months [4].

For the sporadic form a wide variety of causes have been proposed, from repetitive traumatic insults [5] to environmental cues such as the chronic and/or single acute to subacute exposition to intoxicant compounds of the organophsphate class [6–8]. In the sporadic form specific environmental triggers for the aetiology remain still elusive for the most cases, anyway some mutations can account for this event. For the familial form many different genetic insults have been characterized. The first mutations associated with ALS was found in the Superoxide Dismutase 1 (*SOD1*) gene [9] and one of its most characterized one is an aminoacidic substitution of a glycine with an alanine at position 93 of the protein (SOD1-G93A). Being a loss of function in a free radical scavenging enzyme, it pinpointed a possible involvement of oxidative stress in the pathogenetic mechanism, but very rapidly with the discoveries of new mutated genes associated with the disease it became clear that it could be only one, and probably marginal, pathogenetic mechanism involved into the degeneration [10]. The vast majority of cases of fALS are due to mutation in *C9orf72*, *TDP43* and *FUS* among others [10]. Clearly many of the proteins found mutated are RNA-binding proteins (RBP), so molecular processes target of these mutation are mostly likely to be involved into RNA metabolism. Other molecular processes involved are protein homeostasis and cytoskeleton regulation, due to mutations in genes like *UBGLN2, SQSTM1* and *DCTN1*.

Of particular interest is the involvement of FUS in the miRNA biogenesis pathway. miRNAs are a class of short non-coding RNAs with broad regulatory functions; unfortunately an alteration of a subset

of genes solely involved in neuronal function has not been demonstrated.

The other major protein often mutated in ALS is TDP43. It is an RNA binding protein and it is believed to cause ALS by both gain and loss of function. Mutations abolishing its function or mislocalization into the cytoplasm cause aberrant splicing [11,12] of its target while its gain of function mechanism seems to rely on its hyperphosphorylation or hyperubiquitination, These post-transcriptional modifications induce TDP43 aggregation which is believed to be toxic [13,14].

C9orf72 expansion accounts for almost 40% of the fALS cases [15], being the most abundantly present form, and 7% of sALS in European population [16], and has a particular nature of pathological mutation.

1.2. Chromosome 9 open Reading frame 72 (C9orf72).

C9orf72 gene possesses three isoforms, v1, v2 and v3, produced by the usage of two alternative promoters and an early stop codon from the partially retained by differential splicing intron 5 [17], instead of the one present into exon 11 (Fig. 1.1). The isoform v2 is the main one and with the v3 can produce the 481 amino acid-long full length protein, the v1 instead ends at the early stop codon and produce the short form which consists of only 222aa.

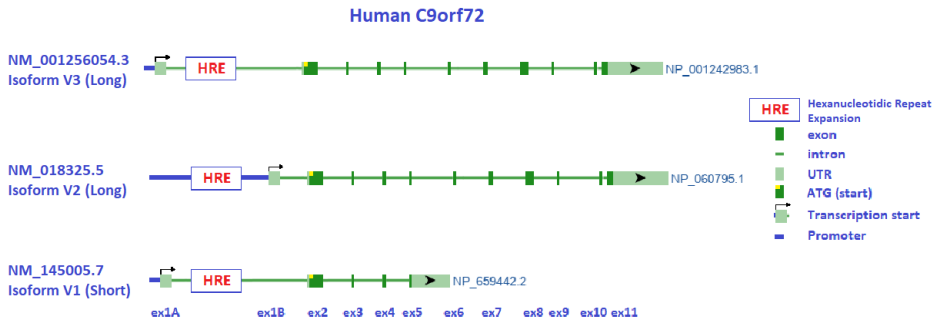

Fig. 1.1 Human C9orf72 transcripts, highlighted features as from legend (sequences lengths not on scale).

Beside its pathological mutation, C9orf72 has been proven to have a physiological role. Human C9orf72 protein shares a very high homology with DENN (differentially expressed in normal and neoplastic cell) and closely related proteins [18], and based on this evidence it is inferred to be guanine nucleotide exchange factor (GEF), which regulates the activity of GTPases [18,19]. It has been shown that C9orf72 protein is present on the lysosomal membrane forming a complex with the Smith-Magenis Chromosome Region 8 (SMCR8) protein [20] and the WD repeat-containing protein 41 (WDR41) protein [21], thus attributing it a role in lysosomal membrane formation and regulation.

Mutations in the *C9orf72* locus are responsible for the majority of familial cases of ALS accounting for 30% of them and 5% of total ALS diagnosed cases [22]. The genomic alteration responsible for the disease is the expansion in number of repeats of a hexanucleotidic sequence GGGGCC embedded into the first intron, surrounded by exon 1a and exon 1b, of the locus as reported almost simultaneously

by two research groups in 2011 [23,24]. It shows a dominant autosomal transmission. This repetitive sequence, when mutated, can reach a very high number of repeats, even more than 400 hundreds [25], and the mutation is defined as Hexanucleotidic Repeat Expanded (HRE), while there is no consensus on the threshold of a non-pathological number, 23 to 30 repeats [25] is somehow considered normal even if the vast majority of individuals possess less than 10 - 11 repeats [16,26]. Since *C9orf72* expression is ubiquitous through all cell types, like many of the ALS-associated genes, the ultimate reason for the specific degeneration of motor neurons cannot be recapitulated by a mere expression alteration. The v2 isoform is transcribed from the exon 1b thus the repetitive sequence lies inside its promoter, while the v1 and v3 isoforms are transcribed by the alternative promoter from the exon 1a, so the repetitive sequence is present into the transcripts.

1.3. C9orf72 pathogenetic mechanisms.

ALS due to *C9orf72* repeat expansion arises because of many mechanisms. First the expanded allele is transcribed in abnormally long transcript. The embedding of the hexanucleotide repeat in these transcripts makes them very repetitive and, due to the high G content, the repeats can fold into a secondary structure called G-quadruplex [27,28]. This structure is held together by Hoogsteen base pairing with hydrogen bond among iminic N7 with the primary amine group in position 2 and carbonyl group in position 6 to secondary ammine group in position 1. This structural feature makes them able to aggregate and precipitate, this process produces RNA foci which are believed to be toxic to some extent. Moreover, this structures can sequester RBP and

other nuclear factors preventing the fulfillment of their normal functions; this point is still controversial since seems that this sequestration is not hindering the cell extensively and contradictory data have been published [29].

The presence of such a high GC content sequence also permits the formation a R-loops during transcription [30], this happens particularly in loci were the high GC content is accompanied with high G skew between filaments [31,32] and repeats into the *C9orf72* locus seem to fit perfectly in this situation. R-loops are a nucleic acid structure in which an RNA stand (mostly newly synthetized) anneal back to the complementary template DNA strand creating a three-stranded structure in which one DNA strand remans unbound [30]. The displaced DNA strand is exposed to a wide variety of biochemical insults leading to single strand break, in addition the annealed RNA strand can create an obstacle to the transcription and the replication machinery. This situation, even if being physiological in certain circumstances and needed for regulatory purposes, can cause single and double strand breaks in the DNA and if not resolved properly can ultimately activate DNA damage response (DDR).

Another canonical pathogenetic feature of *C9orf72*-ALS is the formation of proteinaceous inclusions. The transcription of expanded allele occurs in both direction, transcripts containing long and repetitive GGGGCC or CCCCGG sequences can undergo a process called Repeat-Associated Non-canonical (RAN) translation in which they are translated in all 6 reading frame. Recently, two distinct

research groups highlighted the presence of a valid Kozak sequence with a cognate CUG codon for translation initiation promoting DPR production [33,34], particularly under stress conditions. This process produces long chain of dipeptide repeats (DPRs) made by the repetition of Pro-Gly, Pro-Arg, Ala-Pro, Gly-Arg, Gly-Pro, Gly-Ala. DPRs can induce cellular toxicity depending on their species, stress status and the presence of many genetic modifiers, even if their toxicity is still a matter of debate [35].

A different possibility is that the HRE causes the disease by a loss-of-function mechanism. The expression of C9orf72 protein is found to be downregulated in post-mortem brains of ALS affected individuals [23], mostly due a lower expression of the V2 transcript [17]. Indeed the HRE causes the hypermethylation of CpG islands in its own promoter lowering the C9orf72 expression [36]. Being involved in the regulation of the autophagy its downregulation can lead to alteration in protein homeostasis [20,37,38].

1.4. ALS disease model and lack of a suitable model.

The field at its infancy investigated the ALS pathology mostly from the clinical or epidemiologic perspective. With the advent of molecular techniques and the genomic era some disease-causing mutations have been discovered and the proper molecular investigation of the pathology started.

Given these premises it became clear that models more amenable to experimental research were needed.

Animal model have been very useful for the investigation of ALS. Mouse model transgenically expressing human SOD1-G93A [39] was the first to shed light on the cellular dysfunction and non-cell-autonomous mechanisms of the disease. It displayed aggressive phenotype with adult onset and short survival, motor deficits and neurodegeneration. Prior to symptoms onset cellular and molecular features are already detectable. These hallmarks are Lewy-bodies and neurofilament-positive inclusions, SOD1 cytosolic aggregation, Golgi apparatus disruption and mitochondrial vacuolation. Beside its benefit this mouse model deals with an instability in transgene copy number which confounds the results in studies which do not account for this alteration.

Some mouse models for *C9orf72*-ALS have also been produced. Mostly haploinsufficiency cannot recapitulate neurodegeneration observed in vivo but showed immune dysfunctions [40]. On the other hand, the possibility to model gain-of-function lays on the expression of exogenous transcript, as done by Chew et al by the overexpression of 66 G4C2 via Adeno-Associated Virus vectors (AAVs); researchers were able to observe also behavioral and cognitive impairment in those mice [41].

A similar strategy has been exploited by O'Rourke et al whom expressed a whole human-derived expanded *C9orf72* gene inside of a bacterial artificial chromosome (BAC). These mice showed RNA foci and DPR due to the presence of the expanded allele accompanied by

mislocalizationg of Nucleolin, pinpointing nucleolar stress, but failed in producing neuronal functional deficit or neurodegeneration [42].

Another mouse model of *C9orf72*-ALS is available [43]. This mouse is based on another BAC into which a patient-derived genomic DNA segment of 98 kb containing C9orf72 gene embedding approximately 1200 hexanucleotidic repeat, has been cloned. It is worth noting that researchers stated in supplementary materials that into the 98 kb of gDNA about 2 kb of the upstream portion of the nearby gene MOB3B without its ATG sequence and part of the genome upstream of *C9orf72* without including other genes are present [43]. Even if it recapitulates many features of *C9orf72*-ALS such as DPR and RNA foci formation, MN loss, TDP43 cytoplasmic aggregation and reduced lifespan, some concern arises on its validity since it shows an incomplete penetrance with sex-related difference where fully penetrant females but not males die at around 6 month and possess an early disease onset.

In 2013 Ciura et al developed a *C9orf72* knock-down strategy in Zebrafish in order to evaluate the effect of haploinsufficiency. The researcher downregulated Zebrafish homolog of *C9orf72* by mean of morpholino oligomers that bind mRNA in the ATG sequence of both the sites used, thus preventing the translation initiation of the protein. Induced motor deficits and axonal abnormalities were promptly rescued by human *C9orf72* mRNA injection. Beside these finding some of the features related to C9orf72 pathology were not present, such as the TDP43 cytoplasmic aggregation, RNA foci and DPR. Unfortunately, many other models implemented in Zebrafish

background suggested gain of toxic function of the products of the expansion translation [44].

The situation is further complicated by the presence of many disease modifying genes. Extensive screening, many of which performed in C. elegans [45], found modifiers of almost any of the canonical disease feature from RNA foci to DPR toxicity. These genes were active player in key cellular processes such RNA metabolism, protein homeostasis mostly involved in protein degradation and autophagy regulation and nucleus-cytosol trafficking.

Nonetheless the efforts and the advancement obtained, an animal model capable to recapitulate all the molecular and phenotypical phenomena has not been established so far. The better chance to model the disease in a dish is nowadays the production of MNs from induced pluripotent stem cells (iPSCs) from patients and comparing them with healthy controls-derived ones or their isogenic corrected counterparts. This allowed to have access to the proper cell type targeted by the disease in the less invasive manner possible. Many paper already published [46–50] exploited this strategy giving rise to new insights in the pathology.

1.5. Induced pluripotent stem cells and iPSC-derived MN model.

Every cell type present in the human body is defined by the specific set of genes it expresses and by the differentiation history it went through which specified its differentiative fate. Beside the zygote, which is the only totipotent cell type, all other cells slowly lost their pluripotency along the differentiation. Reversion of this process can be

achieved by the transient expression of some genes, known as pluripotency factors, and has been achieved for the first time by Takahashi and Yamanaka in 2006 with the set of Oct3/4, Sox2, c-Myc, and Klf4 genes [51]. The cells obtained by this process are termed iPSCs (Fig. 1.2.). Most importantly these cells bear the same patient's genotype which allows to use them to model patient's disease as well as its own individual variability. Furthermore, iPSCs can be differentiated in almost every cell type present in the body by applying the proper protocol, granting access to tissue which otherwise won't be easily accessible. In the framework of ALS, the degenerating cells are MNs, so the only access point to the disease targeted tissue is at the post-mortem stage rising technical and ethical issues. A new research paradigm has been established after this technical achievement in which patient's cells are collected with a minimally invasive technique and are turned to iPSCs by transduction and transient expression of pluripotency factors and then differentiated into the proper cell type, in our case MNs. Thanks to iPSCs we can now produce patient-specific MNs in a dish to be used for research.

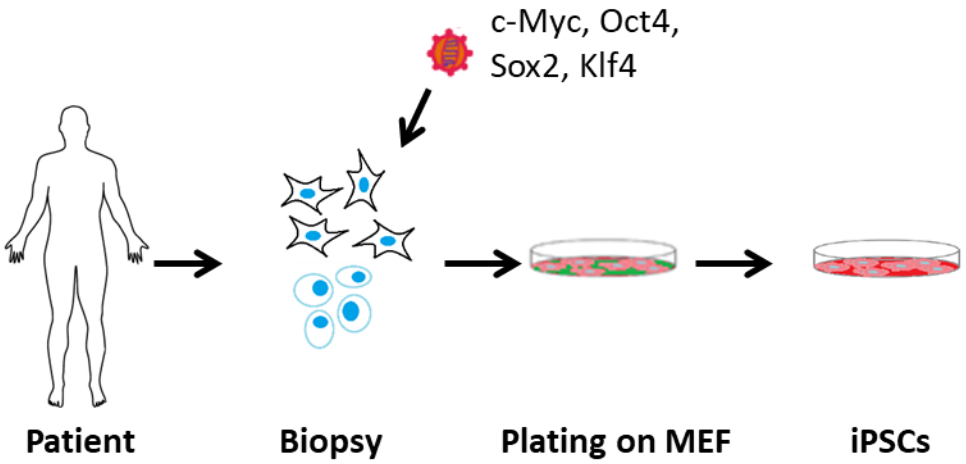

Fig. 1.2. Reprogramming patient's cells into iPSCs.

For our purpose we need to study the hallmarks of *C9orf72*-ALS so our differentiation protocol aim to obtain MN, in particular the protocol we chose a protocol from Maury et al [52], which has been partially modified, produces a population of MNs (Fig. 1.3).

Cells reprogrammed to iPSCs grow in adhesion and need to be plated on specific coating, which helps them to maintain their undifferentiated state, if adhesion is avoid, they form small round aggregates by their self- organizing ability. These aggregates are called embryoid bodies (EBs) since they let clustered iPSCs to recapitulate some of the transformation cells go through during embryogenesis. At this stage, iPSCs are capable to produce any of the three germ layers present in the embryo and in absence of external stimuli they naturally produce ectoderm, process which can be pushed furthermore by dual SMAD inhibition. Dual SMAD inhibition is accomplished using small molecules acting as BMP inhibitor and TGF-β inhibitor blocking

downstream signal transduction through BMP and Activin/Nodal signaling which induce mesodermal and endodermal differentiation [53,54], this results in promoting the neuralization of the pluripotent stem cells. Next, the rostro-caudal identity is induced to be more caudal by applying Retinoic Acid, which is the molecule driving the rostro-caudal gradient, in order to drive the differentiation of prospective neuron into a spinal-cord like type, and then the differentiating cells are forced into a ventral fate by adding molecules inducing Sonic-Hedgehog signaling resulting in a ventral spinal cord-like cell type, thus cholinergic MNs. After these differentiative steps neurotrophic factors are applied to maintain MNs identity and mature EBs can be dissociated and plated on poly-Ornithine/laminin coated dishes, mimicking MNs resident environment.

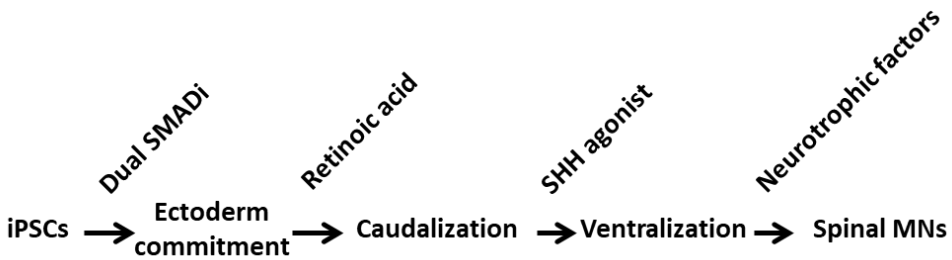

Fig 1.3. Schematic representation of the differentiative steps from iPSCs to iPSC-derived MNs.

1.6. Organoid model.

In vitro cell culture is a powerful tool to investigate diseases and the ability to grow and analyse specific cell types is at the base of our pre-clinical researches. However, specific human features cannot be

reproduced in models, such as the reciprocal contact interaction between cells and their networks.

To overcome these limitations recent advancements have been made by the establishment of 3D culturing techniques. The 3D environment is recreated by a differentiation process which is not confining the cellular identity to a single cell type, thus the cellular variety present in a complex tissue can be modelled better.

In this regard, the most valuable 3D culturing tool is the usage of human organoids. For the investigation of neural pathology, such as the one needed for research on neurodegenerative diseases, the turning point has been the production of neural organoids achieved by Lancaster et al in 2013 [55]. Starting from iPSCs and following steps similar to the ones undertook in neural development, iPSCs can form an aggregate of differentiating cells which will produce many cell types present in the developing brain, reproducing also some features of the 3D architecture of interaction between neurons, astrocytes and glial cells. With some modifications, also brain specific sub-areas can be recapitulated. The round aggregates of cells first move towards ectodermal differentiation and then, thanks to their self-organizing property, start to specify an outer layer of neuroepithelium, which, with the progress of maturation states, can give rise to different mature neural populations and even form folds into the neuroepithelial layer resembling circumvolutions during the neuroepithelium expansion phase. Inside the organoids, neural rosette-like structures can be seen with a proliferative immature precursor area in the inside encapsulated

by a layer of more mature differentiating neurons. This process in accompanied in parallel by the differentiation of the cell types into the neural lineages. The maturation of neurons can be followed by monitoring the changing in morphology, with the shedding of projections that will become the future axons, and by staining for their differentiation stages markers like PAX6 and SOX2 for early precursors and later TUBB3 and Doublecortin for mature neurons or Neurofilament Heavy chain (SMI32) for MNs. At the very late stages, this model is able to recapitulate also the formation of cortical structure producing layer 6 and 5 from the starting sheet of neuroepithelium. This process can be followed by expression of markers TBR1 and Ctip2 for layer 6 and 5, respectively. It seems that the layer 4 cannot be produced autonomously by this model since its specification requires thalamic innervation to guide the specification, thus requiring the presence of specific subset of cell undertaking thalamic differentiation and performing their inducing function, these cells do not form spontaneously by this protocol.

For our purposes we adopted the Lancaster protocol for un-regionalized neural development, known as whole brain, and modified it to obtain a more caudal and more ventral cell type specification producing a spinal cord organoid. This allow to recreate an organoid enriched in spinal MN bearing the features present *in vivo* accounting for 3D structure and non-cell autonomous interaction important for the disease to be modelled.

1.7. Morpholino oligomers.

Many ways to regulate gene expression exists. One of the most used to downregulate expression of target genes is RNA interference (RNAi) by means of short RNA oligomers. This technique relies on the introduction of short interfering RNAs (siRNAs) which bases pair with target mRNA and are recognized by the nuclease DICER with cleaves the mRNA preventing its transcription and inducing its degradation. The RNA should bear the antisense sequence of the target mRNA, thus oligomers like these are known as antisense oligomers (ASOs). This is still a very powerful methods used for research, but it has some features which hinder its usage in an in vivo or therapeutic setting. First of all, the delivery of the oligomer will be difficult in an animal model, for this expression vectors are needed. Second, the RNA introduced is not very stable since it is promptly targeted by endogenous RNAses. To overcome these issues, a different polymer can be used. Phosphorodiamidate Morpholino oligomers (PMO or simply Morpholinos) are a valid alternative. Their phosphorodiamidate backbone, as opposed to the sugar-phosphate of ASO, cannot be cleaved by endogenous nucleases making this ASO more stable. Moreover, these molecules do not induce the cleavage of target mRNA but they base-pair with them competing with the endogenous processing machinery. This feature is useful since it can be exploited to block the binding with splicing factors, manipulating the splicing profile of the RNA of interest, a downregulation is also achieved since the translation process is prevent by the binding of the MOs with the mRNA.

Many ASO-based strategies have been exploited to counteract pathogenetic mechanisms. Also, in the framework of *C9orf72*-related ALS a plenty of ASOs targeting different sites in the locus have been published.

Extensive targeting of *C9orf72* transcript with ASO has been evaluated by Lagier-Tourenne et al [56]. They reported ASO targeting both sense and antisense *C9orf72* transcript reporting. Using ASO targeting sense strand they were able to reduce RNA foci without hindering *C9orf72* mRNA levels, in contrast with siRNA treatments which reduced *C9orf72* mRNA expression level without interfering with nuclear RNA foci.

More recently Sareen et al [48] could reduce the transcription of repeat-containing isoforms by ASO treatment in an attempt to remove the upstream players of toxic mechanism, namely RNA foci and DPR production.

Both former studies [48,56] stated that sustained knock-down of *C9orf72* is not detrimental for the cell while both pointed out that RNA foci participate to the pathology by a gain of function mechanism in which they interact with various RNA binding proteins.

2. AIM OF THE STUDY.

Amyotrophic Lateral Sclerosis is a neurodegenerative disease without any effective cure. Research is hindered by the lack of a reliable models that can recapitulate pathological processes acting in the affected individuals. Indeed, no satisfactory animal model is available for *C9orf72*-related ALS at the moment. As refinement of cellular models, induced Pluripotent Stem Cells (iPSCs) can be useful. Being derived directly from the patient, they possess the same genetic background, can be differentiated in the specific affected cell type (motor neurons (MNs) in case of ALS) and, as it has already been demonstrated, they present canonical *C9orf72* molecular features such as RNA foci and DPR production.

Therefore, iPSCs and iPSCs derived-MNs can be used to investigate pathological alterations and to analyse neuronal specific hallmarks. Moreover, they can be used to test potential therapeutic approaches.

However, iPSC-derived MNs still represent an artefact model in which neurons are deprived of their surrounding environment and interactions with different cell types. To overcome this limit, organoid model has been proposed. Indeed, it can mimic complex systems, such as the structure of brain and spinal cord, can sustain the differentiation better and for longer time then traditional 2D cell culture allowing a more mature differentiative state, which could be the key to model disease with late onset phenotype as ALS.

Given the lack of a suitable model able to fully recapitulate all the pathogenic features present in *C9orf72* ALS, in this study:

- we exploited iPSC technology and iPSC-derived MNs to model the disease and investigate the canonical hallmarks of the pathology;
- we searched for novel useful pathological molecular markers using them as a paradigm to evaluate and test the efficacy of new therapeutics, in particular antisense oligonucleotide-based approach;
- we generated organoid-based models to study if the most complex disease features can be reproduced.

Overall, this study validates transversally the three models analysed and points out new interesting molecular hallmarks to investigate the pathological processes and the response to therapeutic approaches.

3. MATERIAL AND METHODS.

3.1. Cell lines and culture conditions.

Induced Pluripotent Stem Cells were obtained reprogramming fibroblasts from biopsies using CytoTune™-iPS 2.0 Sendai Reprogramming Kit (Invitrogen) according to manufacturer instructions.

Fibroblast from biopsies were maintained in DMEM high glucose, with sodium pyruvate and 200 mM Glutamine (Euroclone) supplemented with 10% FBS, 1% Amphotericin B (Euroclone) and Penicillin/Streptomycin, subsequently fibroblasts were transduced with CytoTune 2.0 Sendai Reprogramming kit (ThermoFisher) according to manufacturer instruction and plated on Mitomycin inactivated Murine Embryonic Fibroblast (MEF) feeder cells. After one-week single colonies showing iPSC morphology were picked and plated in iPSC growing conditions (see below).

C9orf72-expanded CS52iALS-C9n6, CS29iALS-C9n1 iPS cell lines and their isogenic corrected pair CS52iALS-C9n6.ISOC3 and CS29iALS-C9n1.ISOT2RB4 iPSC lines where purchased from Cedar Sinai.

iPSCs were cultured in Essential 8 (ThermoFisher) in Cultrex® Reduced Growth Factor Basement Membrane Matrix, Type 2 (BME 2) (Trevigen) coated dishes, changing medium at least three times a week. Passaging was performed by colony picking or detaching cells with UltraPure 0,5 mM EDTA (Life Technologies) in PBS (KCl 2,7 mM, Na_2HPO_4 8,1 mM, NaCl 136,9 mM, KH_2PO_4 1,5 mM).

MNs derived from iPSCs were cultured in 20 µg/ml Poly-L-ornithine (SigmaAldrich) and 5 µg/ml Laminin from Engelbreth-Holm Swarm murine sarcoma (SigmaAldrich) coated dishes in complete N2B27 medium (see Differentiation section) changing medium every 2-3 days.

3.2. Differentiation protocol.

MNs were obtained via embryoid bodies (EBs) formation as in [52] with few minor modifications.

N2B27 medium was made according to the following recipe. Neurobasal (Life Technologies) and ADMEM/F-12 (Life Technologies) 1:1 mixture was the basal medium and it is supplemented with 1% Penicillin/Streptomycin (Euroclone), 2 mM L-Glutamine (Life Technologies), 0,2 mM β-Mercaptoethanol (Gibco), B27 minus Vitamin A supplement (Life Technologies) and N2 Supplement (Life Technologies).

On Day 0 iPSCs were plated on non-treated dishes, allowing for EBs formation, in N2B27 with 10 µM Y-27632 (Cell signalling Technologies) as anti-apoptotic, 0,1 µM LDN 193189 (Stem Cell Technologies), 20 µM SB431542 (Sigma Aldrich), 3 µM CHIR99021 (Sigma Aldrich) for the ectodermal induction by Dual SMAD Inhibition. Passaging and changing medium were performed letting EBs to settle down and removing supernatant. On Day 2 medium was changed with fresh N2B27 supplemented as before without Y-27632 but adding 100 µM Retinoic Acid to start the ventralization. On day 4 the same procedure was repeated and N2B27 was the same as before without

CHIR99021 but with 500 nM of Smoothened Agonist (SAG, Merck Millipore) as Sonic Hedgehog's pathway activator inducing ventralization. On Day 7 Dual SMAD Inhibition was stopped and N2B27 was supplemented only with 100 nM Retinoic Acid and 500 nM. On Day 9 the medium was as the previous timepoint but adding 10 µM DAPT (Stem Cell Technologies) to indirectly inhibit Notch signalling. On Day 11 neurotrophic factor treatment started by adding 10 ng/mL BDNF (Peprotech) and 10 ng/mL GDNF (Peprotech), from this day the N2B27 was considered complete motor neuron medium and it was used for further culturing. Motor neurons could be dissociated from Day 9 but as standard protocol the dissociation was on Day 14.

EBs were collected and centrifugated at 300 g for 5 minutes, supernatant is removed, pellet was washed with 8 mL PBS and centrifugated at 300 g for 5 minutes again. Supernatant was removed and EBs were suspended in 4,5 mL PBS and dissociated adding 0,5 mL Trypsin 2,5% (Gibco) incubating at 37°C for 5 minutes. Dissociation was blocked by adding 2 mL of sterile FBS (Euroclone) and pellet was collected by centrifugation at 300 g for 5 minutes. Dissociated pellet was resuspended in N2B27 complete medium supplemented with 10 µM Y-27632 for cell counting. Dissociated MNs were plated at 0,5*10^5 cell on poly-L-ornithine/Laminin-coated coverslip or well of 24-well plates or 0,2*10^6 cells each of poly-L-ornithine/Laminin-coated well of a 6-well, the medium was changed 24 hours after dissociation to remove Y-27632 and expression of MN markers were assessed by immunofluorescence.

Analysis were performed at least after day 16 from the start of the differentiation protocol.

3.3. Morpholinos treatments.

Morpholino oligomer A (MOA) and Morpholino oligomer B (MOB) were purchased from GeneTools Inc in lyophilized formats, suspended in sterile water and stored at 4°C, sequences are listed in the Antibody and Oligos section.

The MO treatment consisted in changing medium with the appropriated one supplemented with 20 µg MO each 1*10^6 of MNs and culturing for 48 hours before removing the treatment and subsequent culturing for additional 48 hours or until the appropriate timepoint for the analysis.

3.4. Gene expression analysis.

RNA was extracted with ReliaPrep RNA Miniprep System (Promega) according to manufacturer instructions. Cells were washed twice with PBS before to be lysed directly in the plate with the lysis buffer from the kit and stored at -80°C until extraction. RNA quantity and quality were assessed by spectrophotometric analysis with NanoDrop One (ThermoFisher) and 260/280 nm and 260/230 nm absorbance ratio evaluation.

Retrotranscription of extracted RNA was performed with the Ready-To-Go You-Prime First-Strand Beads (GE Healthcare) using from 100 ng to 5 µg of RNA producing cDNA stored at -20°C for gene expression analysis.

Gene expression was quantified by real-time qPCR on 7500 Real-Time PCR System (Applied Biosystems) with TaqMan molecular probes or standard primer-based SYBR green detection with and their respective commercially available TaqMan™ Universal PCR Master Mix (Applied Biosystems) or Power SYBR™ Green PCR Master Mix (Applied Biosystems). Cycle threshold were normalized on reference gene and fold change were calculated by ΔΔCt method.

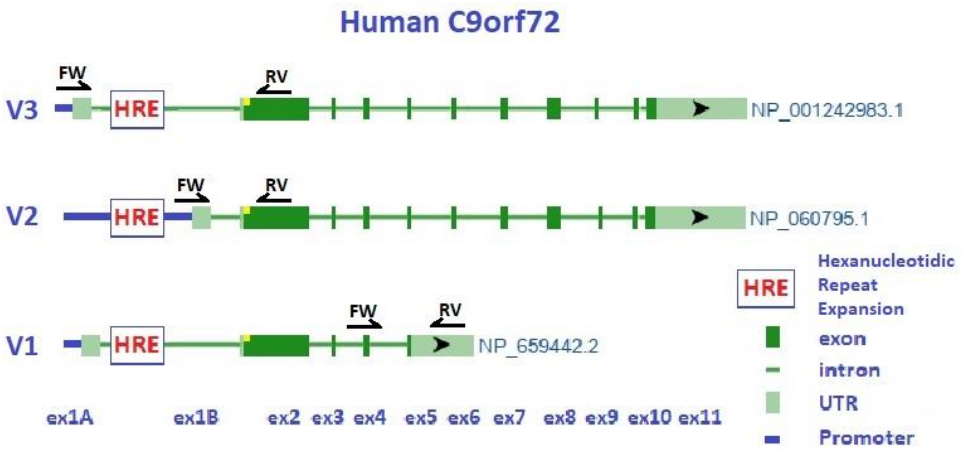

Fig. 3.1. Real-time qPCR primer positioning for *C9orf72* isoform quantification.

3.5. RNA foci and DPR measurements.

The DPR measurement was performed by Dr. Tania Gendron at Mayo Clinic with proprietary ELISA-based method able to detect (GP)n repeats. Samples for this assay were constituted by dry cell pellet and it was collected as follow. Once the iPSCs or iPSC-derived MNs were ready to be collected they were washed twice in PBS and detached by incubation with EDTA 0,5 mM in PBS for 5 minutes or until cells observed under the microscope appear to detach or the edges of the

colony starts to curl up. EDTA was removed and cells were recovered with fresh medium or PBS. Then cells were centrifuged at 300 g for 5 minutes, washed once with PBS and centrifuged at 300 for 5 minutes again. Supernatant was totally removed drying the pellet which was stored at -80°C. Samples were shipped in dry ice for quantification of the DPR. RNA foci analysis by fluorescence in-situ hybridization has been performed as previously described [57] by Dr. Clara Volpe at Istituto Auxologico in professor Antonia Ratti's laboratory.

3.6. Immunofluorescence.

Once cells were at appropriate confluency or the timepoint was reached cells were washed twice with PBS, fixed with PFA 4% for 10 minutes at room temperature and washed three times to remove residual PFA. Coverslips could be stored at 4°C leaving the third wash or immediately processed. Permeabilization/fixation was performed with 0,3 Triton X-100, Normal Donkey Serum (Jackson ImmunoResearch) or Normal Goat Serum (Jackson ImmunoResearch) matching the specie of the secondary antibody to be used, in PBS for 1 hour at room temperature. Coverslips were incubated with primary antibodies mix at appropriate dilution over night at 4°C. Antibodies were removed and samples were washed three times with PBS for 5 minutes and incubation with fluorophore-conjugated secondary antibodies mix at appropriate dilution in PBS for 1 hour and 30 minutes at room temperature in the dark. Excess of antibodies was removed with three PBS washes as before and nuclei were counterstained incubating coverslips with DAPI 1:1000 in PBS for 10 minutes in the dark. After three additional PBS washes

coverslips were mounted on slides with FluorSave (Merck Millipore), dried overnight in the dark at room temperature and then stored at -20°C in the dark until imaging.

Negative controls by staining with only secondary antibody without primary one have been performed for every secondary antibody on iPSCs and iPSC-derived MNs.

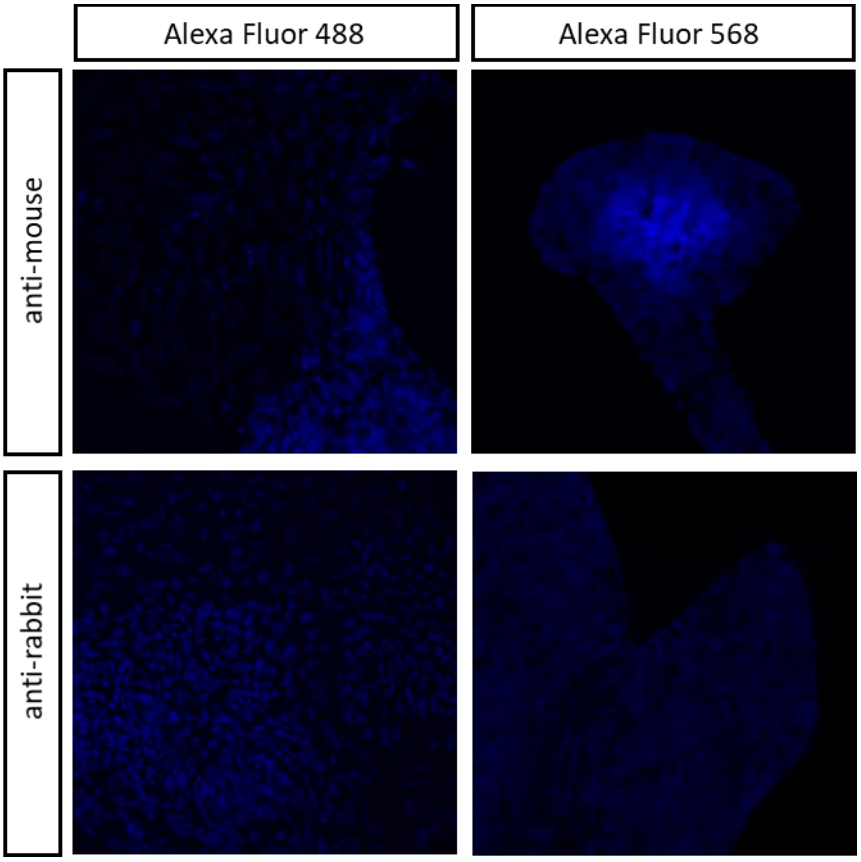

Fig. 3.2. Representative images of negative control staining with only secondary antibodies on iPSCs.

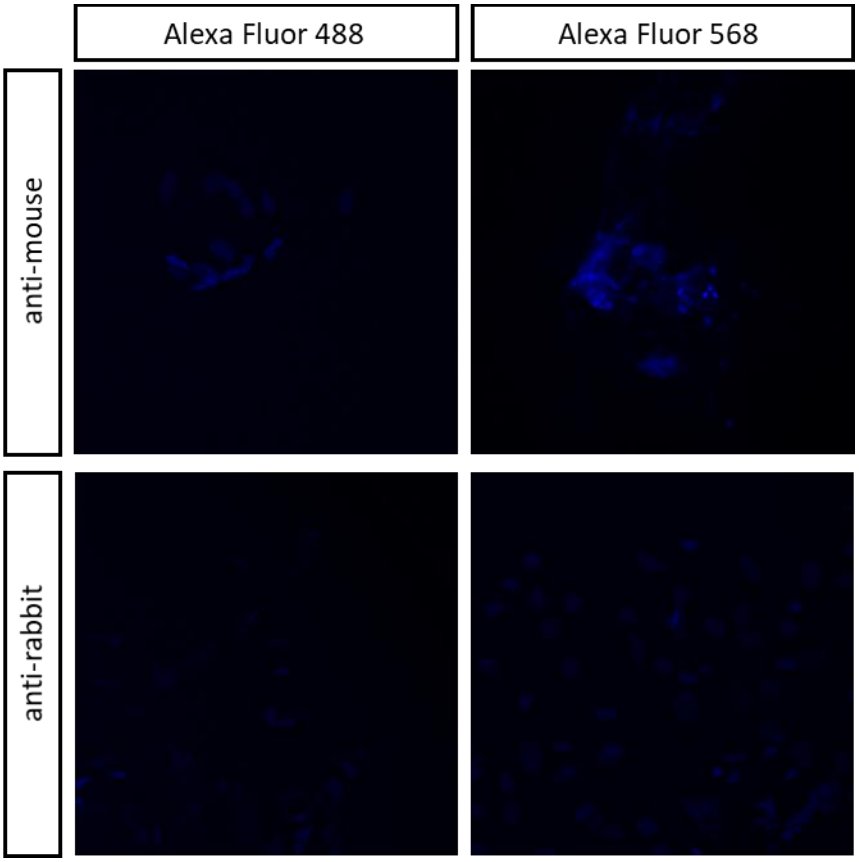

Fig. 3.3. Representative images of negative control staining with only secondary antibodies on iPSC-derived MNs.

3.7. DNA damage markers quantification by immunofluorescence.

Images were acquired with Leika DMi8 confocal microscope and were processed for quantification as follow.

Using ImageJ software, in its Fiji distribution (Fiji is just ImageJ), images were open and split into their constituent channels, on the channel for DAPI staining nuclei were segmented by thresholding with manual selection if need, this yielded an 8-bit binary version of the image and ROI were selected with built-in function. Once defined the

ROIs they were applied on the channel in which the DNA damage marker was stained and selected and quantified by Analyze particles and its measurement functionality. Statistics were applied on the IntDen (integrated density) parameter.

3.8. Motor neurons lengths measurements.

Images were acquired with same acquisition procedure as before. Neuronal identity was assessed using SMI32 antibody for visualization and lengths were measured semi-automatically on 8-bit images with NeruonJ plugin of ImageJ software. Distances were not calibrated so the measurements are in arbitrary units.

3.9. Organoids production protocol.

Brain organoids were produced as in Lancaster et al [58], for spinal cord differentiation the protocol was the same but small molecules were added as stated.

The first medium used was hES made as follows, DMEM/F-12 (ThermoFisher) supplemented with 20% Knock-out Serum Replacement (Gibco), 3% Fetal Bovine Serum (Euroclone), 2 mM L-Glutamine (Gibco), 1% MEM-NEAA (Gibco), 0,17 mM 2-β-Mercaptoethanol (Gibco).

On day 0 iPSCs were detached with Accutase (Stem Cell Technologies) incubating at 37°C for 4 minutes, collected, spun at 270 g for 5 minutes, suspended in hES for counting and plated at 9000 cells/well in 96well Ultra-low attachment plate in hES supplemented with 50 µM Y-27632, 1,6 µg/mL bFGF.

Changing medium were performed removing partially the medium and replacing it with fresh one every 2 days until day 6, on day 4 Y-27632 and bFGF supplementation were stopped.

On day 6 organoids were transferred in 24well Ultra-low attachment plate using the p200 pipette with cut tip using 500 µL each well of Neural Induction Medium (NIM) constituted as follows, DMEM/F-12 (ThermoFisher), 1% N2 Supplement (Gibco), 1% Glutamax (Gibco), 1% MEM-NEAA (Gibco), 1 µg/mL Heparin (Sigma Aldrich). On day 8 500 µL of fresh NIM were added and on day 10 medium was replaced with fresh NIM.

On day 12 organoids were embedded in ECM Gel from Engelbreth-Holm-Swarm murine sarcoma droplets at 37°C for 1 hour and then transferred into 60mm dishes in Matrigel medium constituted as follow, 1:1 mixture of DMEM/F-12 (ThermoFisher) and Neurobasal (ThermoFisher), 1% Penicillin/Streptomicin (Euroclone), 1% Glutamax (Gibco), 1% B27 minus Vitamin A supplement (Gibco), 0,5% NEM-NEAA (Gibco), 0,5% N2 supplement (Gibco), 0,17 mM 2-β-Mercaptoethanol (Gibco) and 1,25 µg/mL Insulin (Sigma Aldrich).

On day 14 organoids were transferred in spinning flask in Flask medium which was made as Matrigel medium with B27 Supplement (Gibco) instead of B27 Minus Vitamin A supplement.

For spinal cord differentiation the same procedure was performed but medium was supplemented with 0,2 µM LDN 193189 (Stem Cell Technologies), 2 µM SB431542 (Sigma Aldrich) and 3 µM CHIR99021 (Sigma Aldrich) from day 2 to day 7 for ectoderm induction. From day

6 medium was supplemented with 100 nM Retinoic Acid (Sigma Aldrich) for caudalization and from day 12 medium was supplemented with 1 µM Smoothened Agonist (SAG, Merck Millipore) for ventralization. From day 28 Retinoic Acid and Smoothened Agonist concentrations were reduced to a half and medium were supplemented with BDNF, GDNF and IGF2 at 10 ng/mL each. Flask medium was changed every week.

At appropriate timepoints organoids were washed three times in PBS, fixed in PFA 4% for 15 minutes at room temperature, washed three times and soaked in 30% sucrose at 4°C overnight. The day after organoids were soaked in 10% gelatin 7,5% sucrose solution at 37°C for 15 minutes and embedded in the same solution, frozen on dry ice and stored at -80°C until cryosectioning for further analysis.

3.10. Antibodies and Oligos.

Antibody	Dilution	Brand	Cat.
Neurofilament heavy chain (SMI32)	1:1000	Biolegend	801701
TUBB3	1:500	Biolegend	801201
Islet1	1:400	Abcam	ab109517
HB9	1:200	Abcam	ab92606
HOXB4	1:100	Abcam	ab133521

γH2AX	1:800	Abcam	ab11174
SOX2	1:500	Abcam	ab97959
Oct4	1:250	Invitrogen	701756
SSEA4	1:100	Invitrogen	41-400
p21	1:100	Abcam	ab109199
BRCA1	1:100	Cell Signaling Technologies	9010
DNA-RNA Hybrid [S9.6]	1:200	Kerafast	ENH001
TDP43	1:200	Proteintech	10782-2-A
Nucleolin	1:1000	Abcam	ab22758

Oligo	Sequence	Application
MOA	TGGTCCTGGTCCTGGTCCTGGTCCT	MOs
MOB	ACATCACTGCATTCCAACTGTCACA	MOs
C9orf72-1F	TCATCTATGAAATCACACAGTGTTC	qPCR
C9orf72-1R	GGTATCTGCTTCATCCAGCTT	qPCR

C9orf72-2F	GCGGTGGCGAGTGGATAT	qPCR
C9orf72-2R	TGGGCAAAGAGTCGACATCA	qPCR
C9orf72-3F	CAAGAGCAGGTGTGGGTTTAGGAG	qPCR
C9orf72-3R	As C9orf72-2R	qPCR
C9orf72-F	ACACATATAATCCGGAAAGGAAGAAT	qPCR
C9orf72-R	TTCTAAGATAATCTTCTGGACATTTTCTTG	qPCR
GAPDH FW	GAAGGTGAAGGTCGGAGTC	qPCR
GAPDH RF	GAAGATGGTGATGGGATTT	qPCR

3.11. Statistical analysis.

Statistical analysis has been performed by t-test with p-value < 0.05 for statistical significance when two variables were compared or by ANOVA with an α-level 0.05 followed by pairwise post-hoc comparison with Tukey correction for multiple testing. Data were collected in three independent experiments if not otherwise stated.

4. RESULTS.

4.1. Induced Pluripotent Stem Cells.

4.1.1. iPSC model characterization and C9orf72 pathological hallmarks.

The iPSCs used in this study have been reprogrammed in our Lab or obtained from cell repositories. To prove their effective staminality, they have been tested for the expression of a panel of stemness markers by immune fluorescence. We analyzed the expression of: OCT4 and SSEA-4. *OCT4* is one of the first pluripotency-related transcription factors to be downregulated upon differentiation [59], while SSEA-4 is specifically expressed on the surface of human stem cells (Fig. 4.1).

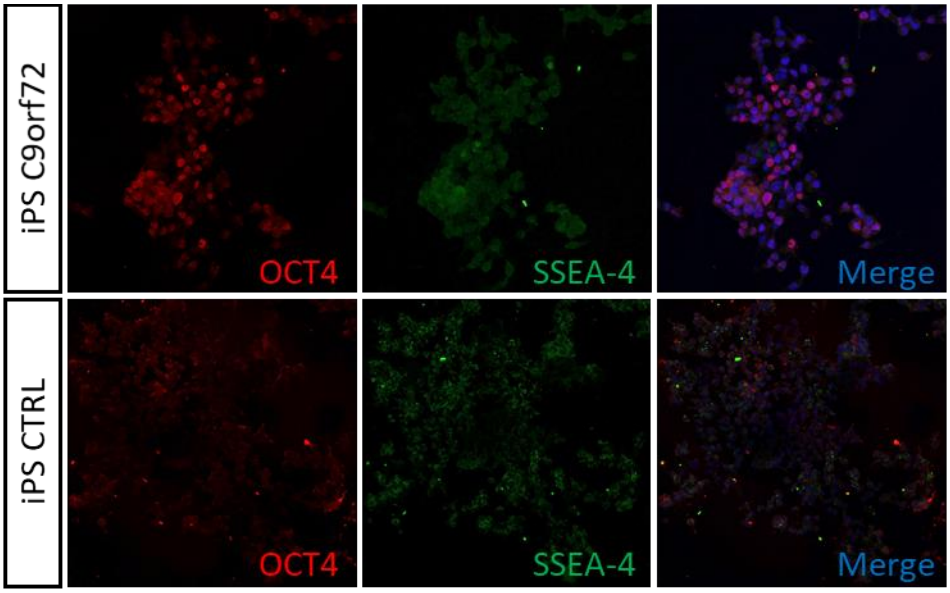

Fig. 4.1. Representative images of OCT4 (red) and SSEA-4 (green) expression revealed by immunofluorescence on iPSCs C9orf72-ALS (first row) and control (CTRL, second row). DAPI, blue signal.

4.1.2. RNA foci and DPR in iPSC model.

A proper disease model is needed to recapitulate the pathological molecular signature of the disease. ALS caused by the expansion of the hexanucleotidic repeats number in the *C9orf72* locus is characterized by the accumulation of foci of aberrant mRNA transcripts produced by the mutate locus and the aggregation of the five species of dipeptide repeats anomaly transcribed by Repeat-Assosicate Non canonical Translation (RAN translation) from these mRNAs. To validate iPSC-based model, we first checked the presence of these molecular disease hallmarks in our iPSCs lines carrying the hexanucleotidic expansion compared to control ones.

Since the locus *C9orf72* is transcribed in both the sense and anti-sense direction, RNA foci are constituted by the aggregation of both the sequences. This allows to monitor the presence of the transcript with Fluorescence In-Situ Hibrydization (FISH) using probe complementary to each strand. Expansion-carrying iPSC lines showed a higher number of cell positive for the presence of RNA foci and a higher number of foci per cell ($P<0.05$) with both the probes, sense and anti-sense compared to controls (Fig. 4.2).

		SENSE FOCI		ANTISENSE FOCI	
Status	Line	%cells foci +	Avg foci N	%cells foci +	Avg Foci N
Expanded	iPS C9_1	14,2%	1,1	26,5%	1,8
Expanded	iPS C9_2	36,1%	2,7	68,2%	2,2
Expanded	iPS C9n1	31,5%	1,7	45,8%	2,9
Expanded	iPS C9n6	20,4%	3,6	33,0%	1,6
Control	iPS C9n6 iso	1,2%	1,0	0,0%	0
Control	iPS CTRL Auxo	0,5%	1,0		

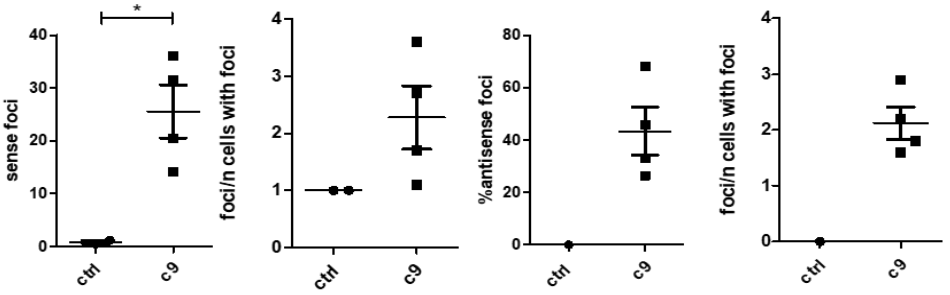

Fig 4.2. FISH-based quantification of RNA foci in iPSC model, plot showing mean ± SEM, Student's t-test, *P < 0.05.

Thanks to ongoing collaboration with Mayo Clinic we quantified the Glycine-Proline DPR in our iPSCs by an ELISA-based assay showing that *C9orf72*-expanded lines have DPR accumulation (P < 0.001, Fig 4.3).

A

Cell Line	Average	StdDev
iPS CTRL 1	130,5	7,78
iPS CTRL 2	135,0	2,83
iPS C9n6 Isogenic	142,5	26,16
iPS C9n6	273,5	2,12
iPS C9n1	1687,5	74,25
iPS C9_1	1905,0	45,25
iPS C9_2	309,0	8,49

B

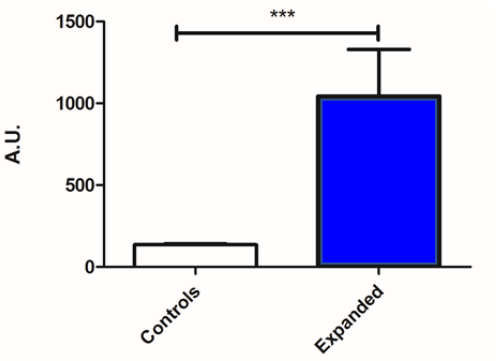

Fig 4.3. ELISA-based quantification of DPR foci in iPSC model. A) table showing raw data. B) Histogram showing quantification of grouped data as *C9orf72* vs controls, Student's t-test ***$P < 0.001$.

4.1.3. DNA damage accumulation and DNA Damage Response alteration.

Numerous evidences have pinpointed an increased level of DNA damage as well as a deregulation of the DNA Damage Response (DDR) pathways in *C9orf72* expanded cells [60]. It is reasonable to investigate if the iPSC model could recapitulate also this pathological hallmark and could be used to investigate new molecular features related to this deregulation. Therefore, canonical DNA damage markers have been analyzed in the iPSCs model. The expression of Breast Cancer Associate 1 (*BRCA1*) and its phosphorylation (*pBRCA1*) as well as phosphorylation of H2AX on Ser-139 are well known to be upregulated in a genotoxic stress situation and in presence of DNA double strand breaks. BRCA1 is a E3 ubiquitin ligase active in DNA damage repair, when phosphorylated by ATM or ATR it acts through its downstream target Chk1 to regulate G2/M cell cycle arrest [61]. The other DNA damage marker analysed is ɣH2AX, it is

another target phosphorylated by ATM/ATR upon DNA damage induction and it is responsible for the creation of a chromatin state which allows for the recruitment at DNA double strand breaks sites of repairing agent such as Rad50, Rad51 and later BRCA1 [62]. By immunofluorescence, these markers can be detected and quantified. Comparing the iPSC lines, it became clear that pathologically expanded iPSCs showed a higher signal ($P < 0.01$ for *γH2AX* and $P < 0.001$ for *BRCA1* and *pBRCA1,* Fig 4.4) compared to the non-pathological ones.

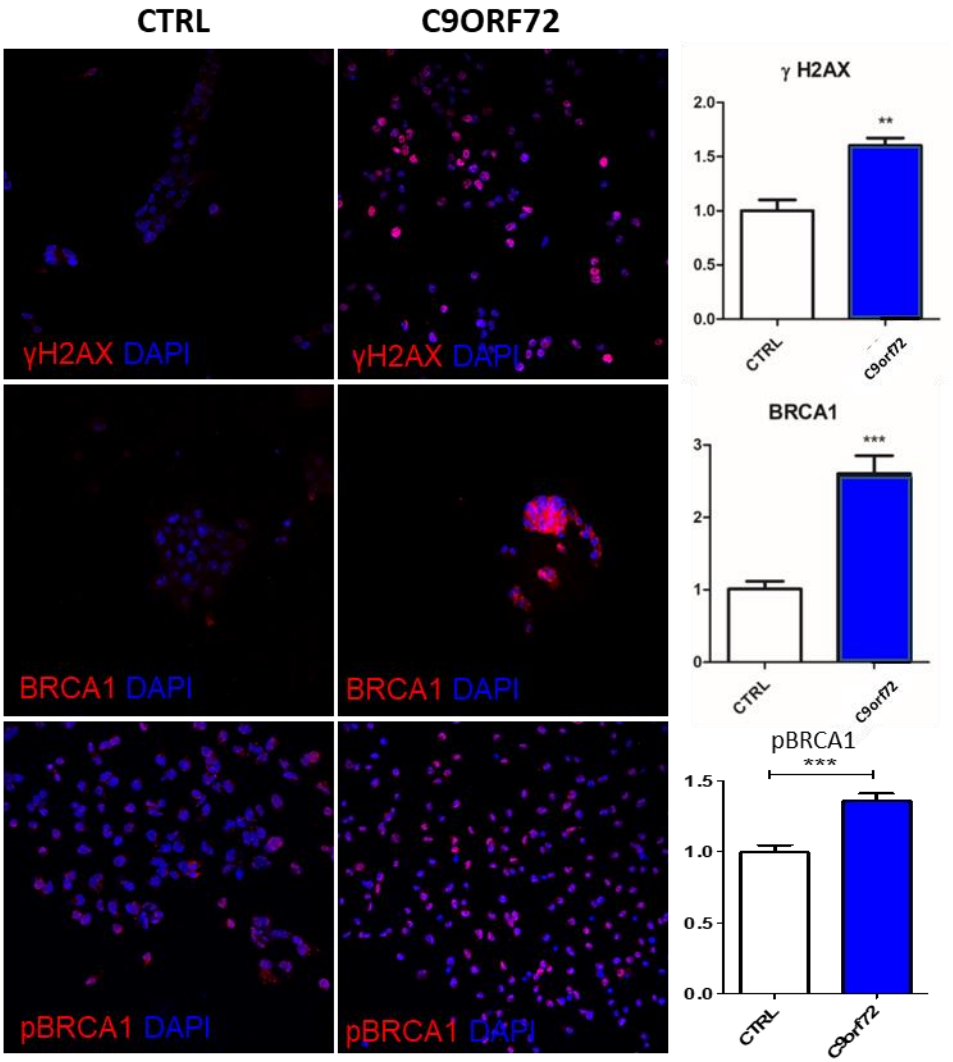

Fig 4.4. Representative images of DNA damage markers analysis by immunofluorescence and their quantifications, normalized on control, in iPSC model. Student's t-test, $^{**}P < 0.01$ for *γH2AX* and $^{***}P < 0.001$ for *BRCA1* and *pBRCA1*.

Presence of genotoxic stress triggers DNA damage response, a complex pathway in which many functionally different proteins interact. Sensors detect the damage, transducers propagate the DDR signal,

while effectors operate to repair the damage. Many genes involved in this pathway can act as markers which expression is regulated upon DNA damage. Among them Growth Arrest and DNA Damage Inducible 45 Alpha (*GADD45a*), Cyclin Dependant Kinase Inhibitor 1A (*CDKN1A* also known as p21) and Sirtuin1 (*SIRT1*) have been selected for analysis.

GADD45a and *CDKN1A* are induced upon DNA damage and they participate into the activation of DDR [63]. SIRT1, among many other roles, recruits to the damage site proteins belonging to NHEJ, HR, MMR pathways and other involved in Nucleotide excision repair and base excision repair pathways and it activate them through its deaceylating function [64]. Therefore, SIRT1 is involved into the recovery after the genotoxic insult. Interestingly, their expression investigated by real-time qPCR showed an upregulation of *GADD45a* and *CDKN1A* ($P < 0.01$ for both genes, Fig. 4.5) in *C9orf72* iPSC lines in respect to controls, coherent with an increased presence of DNA damage, while *SIRT1* level did not change ($P = 0{,}765$, Fig. 4.5).

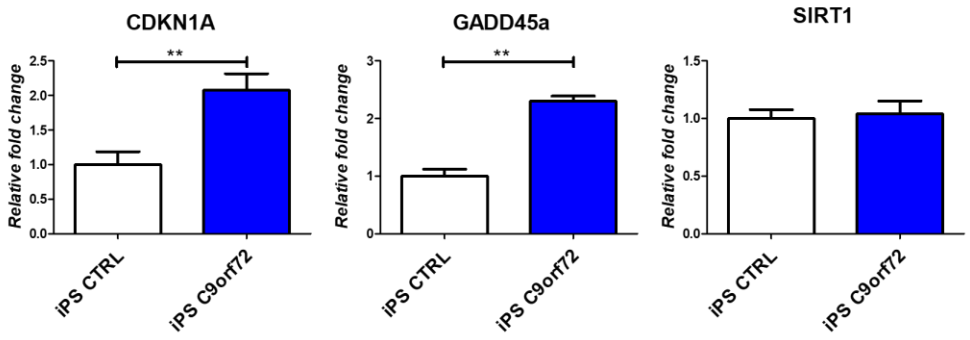

Fig. 4.5. Gene expression, normalized on control, of DNA damage markers. *CDKN1A* and *GADD45a* (**$P < 0.05$ for both genes) and *SIRT1* (not significant).

4.1.4. R-loops in iPSC model.

The structure called R-loops is formed by three stranded nucleic acid in which the newly transcribed RNA anneals back to the template strand level. These structures are not pathological per se but need to be finely regulated since are prone to cause DNA damage. By staining with the S9.6 antibody, which recognize these nucleic acid structure, R-loops could be detected and quantified, taking into account that R-loops constitutively present in rRNA loci (Nucleolin signal) need to be excluded, because they can mask S9.6 signal.

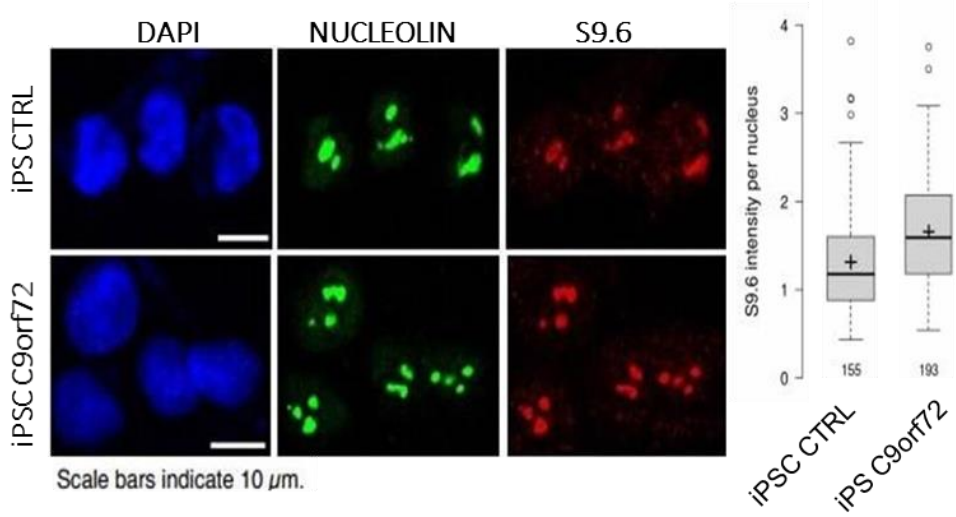

Fig. 4.6. Immunofluorescence image staining for R-loops (red), *NUCLEOLIN* (green) and DAPI (blue). Image quantification.

Quantification of R-loops showed increased accumulation of these structure in C9orf72-expanded iPSCs, even if not statistically significant (Fig. 4.6).

4.1.5. Anti-sense Morpholino oligomers rescue of pathological hallmarks in iPSC model.

The data collected so far showed that iPSCs were able to recapitulate molecular pathological hallmarks of the *C9orf72* related ALS. As a proof of principle, a treatment with phosphorodiamidate morpholino oligomer (MO) targeted against the expansion should reduce DPR production, blocking their downstream effects and reverting the hallmarks analysed.

At this purpose two MOs, designed by GeneTools LLC, were used: MOA and MOB, targeting the ATG at translation start site in the exon 2 and the hexanucleotidic expansion of the *C9orf72* locus respectively. In MOB sequence mismatches were allowed in order to prevent the formation of G-quadruplex and to be able to bind both sense and antisense transcripts of the HRE.

iPSCs from *C9orf72*-expanded lines have been treated with both MOs and the accumulation of DPR and expression of the same genes used as DNA damage markers were probed. After treating iPSCs with both MOs, data showed a reduction of DPR statistically significant for MOB treatment ($P < 0.05$, Fig. 4.7), a reduction to levels comparable with controls of gene expression of DNA damage markers *GADD45a* ($P < 0.01$, $P < 0.001$, MOA and MOB respectively), *CDKN1A* ($P < 0.01$, $P < 0.001$, MOA and MOB respectively) and a decrease of *SIRT1* upon

MOB treatment ($P < 0.01$, in respect with both controls and *C9orf72* untreated) as measured by qPCR in MOs treated iPSCs (Fig. 4.7).

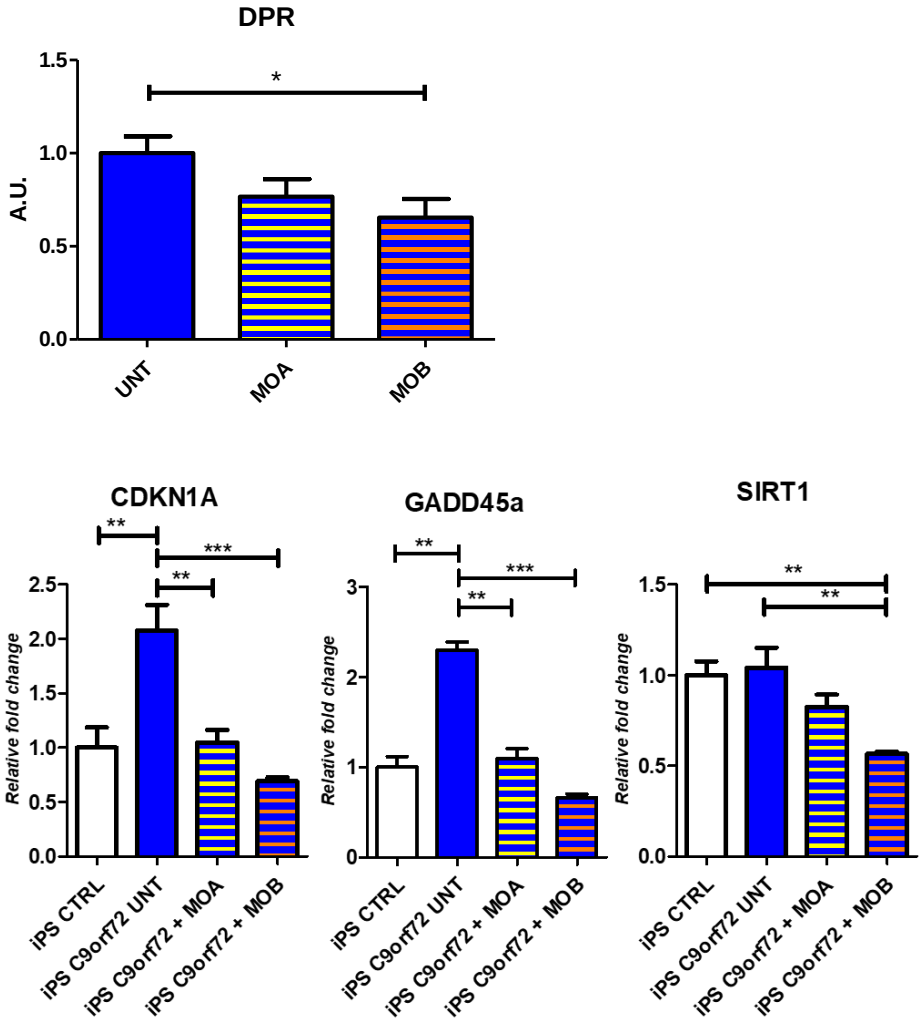

Fig 4.7. DPR (upper, Tukey-corrected ANOVA, * $P < 0.05$, normalized on UNT) and DNA damage markers by real-time qPCR (lower, Tukey-corrected ANOVA, ** $P < 0.01$ in C9orf72 UNT vs controls and C9orf72 UNT vs MOA-treated, *** $P < 0.001$ for C9orf72 UNT vs MOB-treated for both *CDKN1A* and *GADD45a*, ** $P < 0.01$ *SIRT1* gene for both controls and C9orf72 UNT when compared with MOB-treated, normalized on control) in iPSC model.

The protein product of the gene *CDKN1A* is p21, iPSC C9_2 and iPSC CTRL 2 were stained by p21 and its expression at protein level was quantified. *C9orf72* expanded iPSCs showed higher expression of the DNA damage marker in respect with controls and the treatment with MOA and MOB could significantly reduce it (Fig. 4.8, $P < 0.001$ for *C9orf72* UNT compared with all the other conditions).

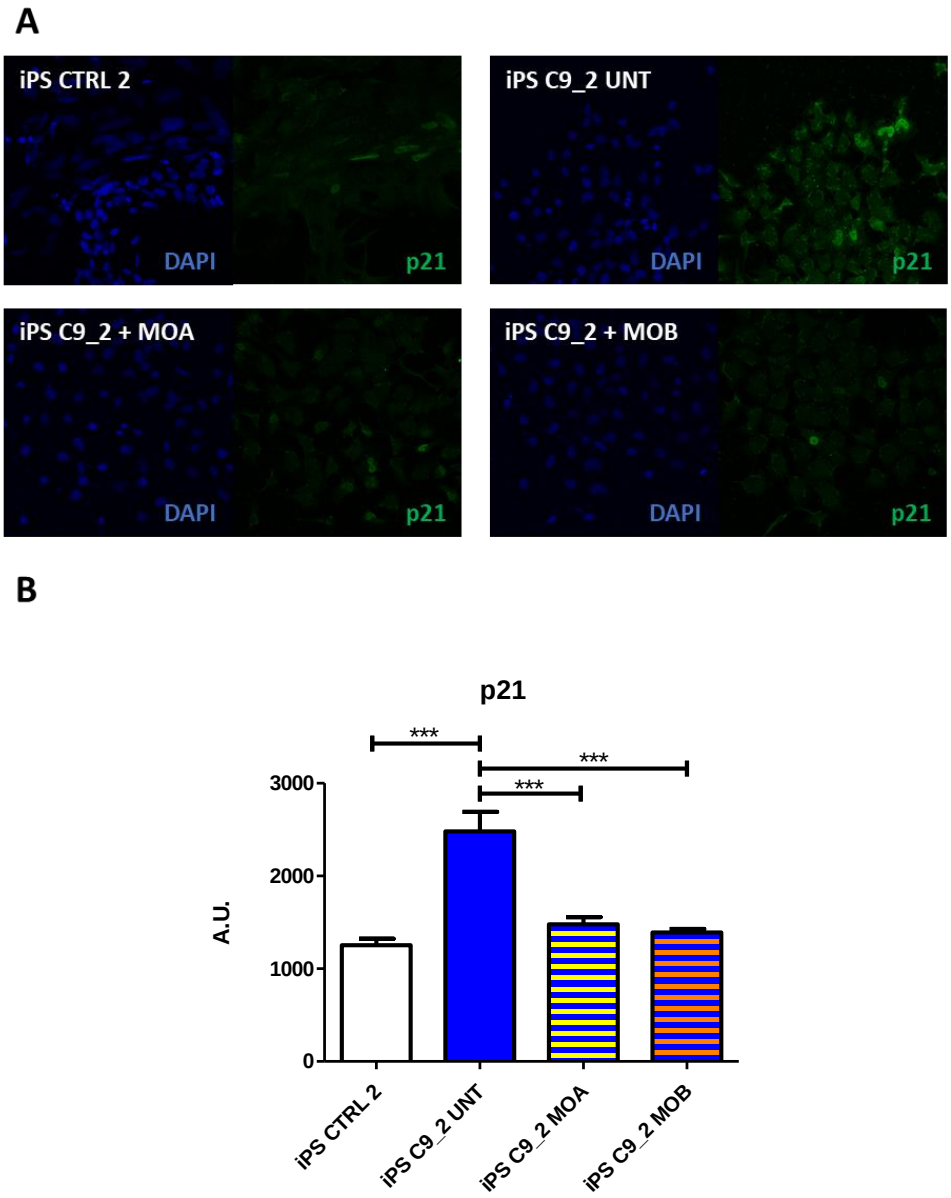

Fig 4.8. A) Representative immunofluorescence images stained for p21 (green) and DAPI (blue). B) Quantification of expression levels by immunofluorescence in iPSC model. Tukey-corrected ANOVA, ***P < 0.001.

Unexpectedly, a reduction of all C9orf72 isoforms expression has been observed upon treatment with both the MOs (Fig 4.9).

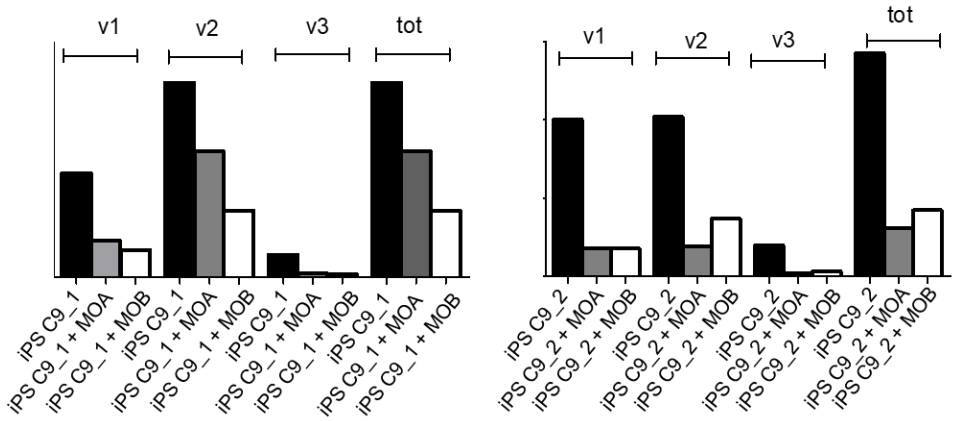

Fig. 4.9. *C9orf72* transcripts expression variation upon MO treatments.

It is known that the presence of the expansion causes the retention of the expanded intron [65], this implies that the variant V3 produced from the pathological allele is not amenable of amplification by primers designed flanking the expansion. The variant V1 and V2 are detected by primer pairs designed far from the expansion.

4.1.6. Global gene expression profiling alteration in ALS iPSC lines and after MO treatment.

Many studies analysed the global changes in gene expression due to *C9orf72* expansion alteration in the framework of ALS. To obtain a clear picture of the global alteration caused by this mutation in iPSCs model a high-throughput direct RNA analysis has been performed. The technique chosen is the Nanostring nCounter using the commercial Neuropathology Panel, comprising 770 genes involved in neurobiology annotated in 23 pathways. RNA extracted from controls,

C9orf72 expanded, and MOB-treated *C9orf72* expanded iPSC lines have been analysed to quantify relative gene expression. After relative quantification statistically differentially expressed genes were grouped for their signaling pathways annotation and used in an enrichment analysis to identify the most deregulated pathways.

It resulted that the mutation in *C9orf72* induced the downregulation of the majority of the pathways analysed in the iPSCs model (Fig. 4.10).

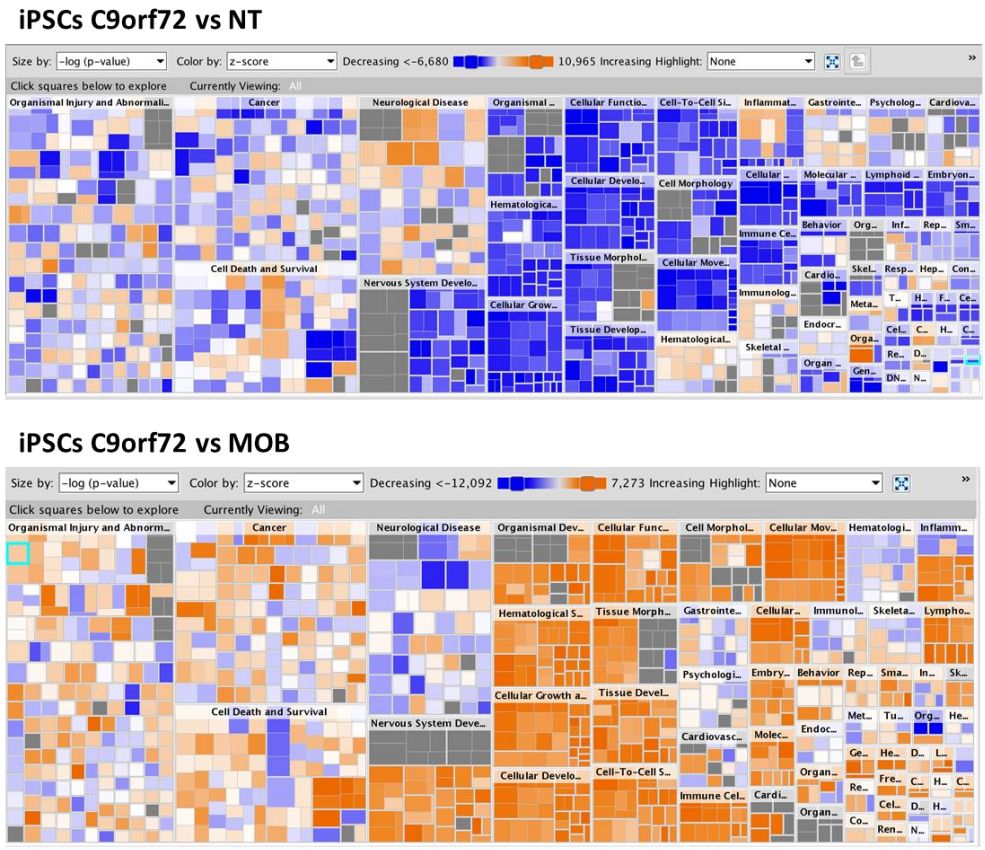

Fig. 4.10. Deregulated pathways in C9orf72 vs NT iPSC, upper. Deregulated pathways in C9orf72 vs MOB-treated iPSC, lower. Orange upregulated pathways and blue downregulated.

Interestingly, many of the deregulated pathways belonged to the regulation of proliferation.

It is worth to note that a downregulated pathway was related to Nervous System Development, this seems to highlight a possible deficit of the priming of iPSC toward neural differentiative fate.

On the other side it became clear that the treatment with MOB could revert this molecular phenotype inducing a recovery of the gene expression in the previously downregulated pathways.

4.2. Induced Pluripotent Stem Cell-Derived Motor Neurons.

4.2.1. Differentiation of iPSCs to iPSC-derived MNs.

The proper cell type targeted by ALS is MNs, both upper and lower. Our differentiation protocol yields a very enriched population of MNs, so after dissociation, between day 17 and day 25, they were used for the analysis.

First of all, the successful outcome of the differentiation protocol has been validated checking the expression of MN markers, in this case we performed immunofluorescence analysis for β-tubulin III (TUBB3), which is a neuronal specific gene, and for HB9 which qualify those cells as MNs (Fig. 4.11).

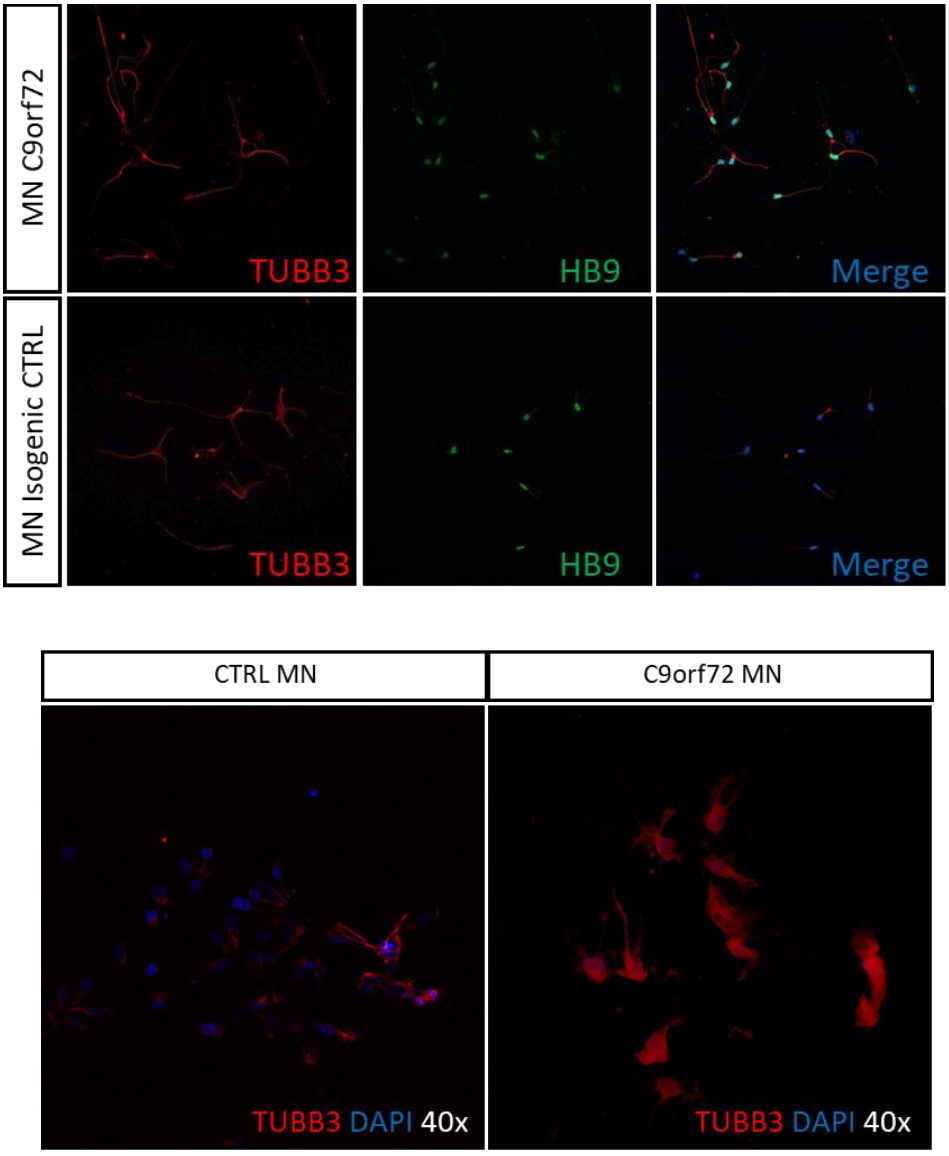

Fig. 4.11. Upper panel: Representative immunofluorescence images of MN markers expression in iPSC-derived MN from lines *C9orf72*-expanded and its isogenically corrected counterpart. Staining for *TUBB3* (red), *HB9* (green) and DAPI (blue). Lower panel: 40x magnification of healthy and *C9orf72*-expanded iPSC-derived MN. Staining for *TUBB3* (red) and DAPI (blue).

4.2.2. RNA foci in iPSC-derive MNs.

The first test to validate iPSC-derived MNs as ALS model is the analysis of RNA foci presence.

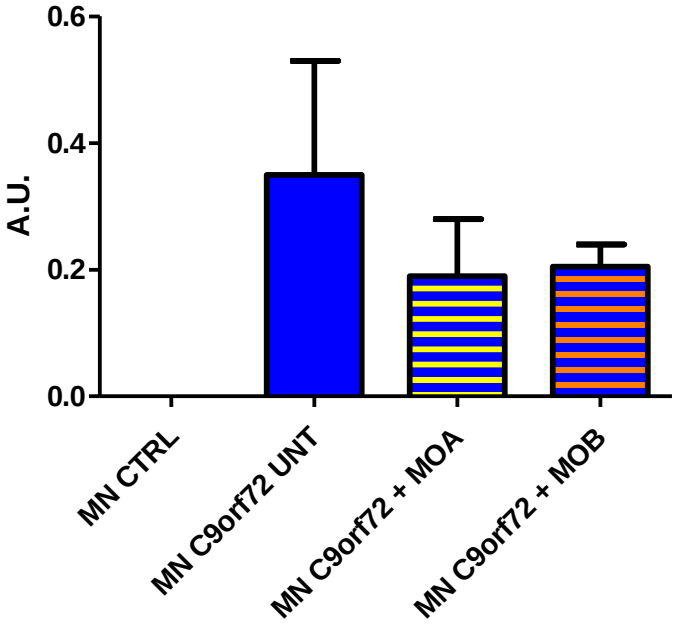

Fig. 4.12. RNA foci quantification in iPSC-derived MNs.

MNs differentiated from *C9orf72* expansion-carrying iPSC lines showed an increased RNA foci levels in respect with controls, levels which are lower in MOs treated samples (Fig 4.12).

4.2.3. DPR accumulation in iPSC-derived MNs.

The same measurement of DPR accumulation performed for iPSCs has been done on iPSC-derived MNs, even if the data are preliminary.

The measurements showed a higher accumulation of DPR in *C9orf72* expanded MNs in respect with healthy controls, data collected on MOs treated *C9orf72* MNs also pinpointed that both MOA and B could be able to induce the reduction of the amount of DPR, in the only cell line analysed, as shown in figure 4.13.

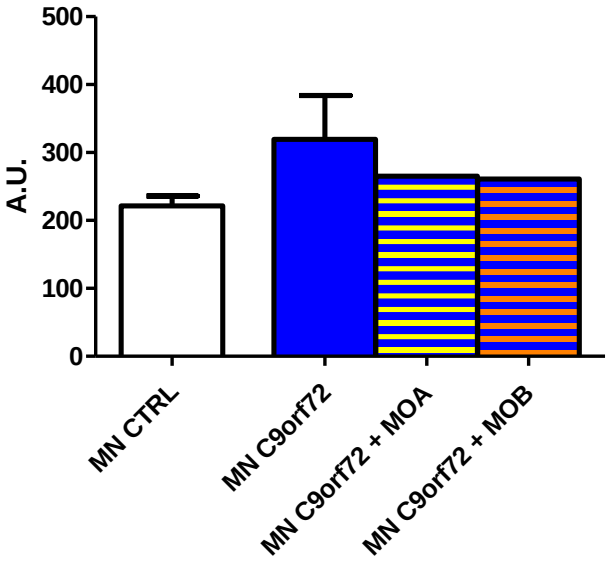

Fig. 4.13. DPR quantification in iPSC-derived MNs.

4.2.4. DNA damage response in MNs.

DNA damage markers have been analysed in iPSC-derived MNs. *γH2AX* expression has been measured by immunofluorescence in MNs derived from *C9orf72* iPSCs and compared with iPSC control-derived ones. Clearly an increase signal ($P < 0.001$) was found in *C9orf72*-MNs suggesting the presence of higher amount of DNA double strand breaks (Fig 4.14).

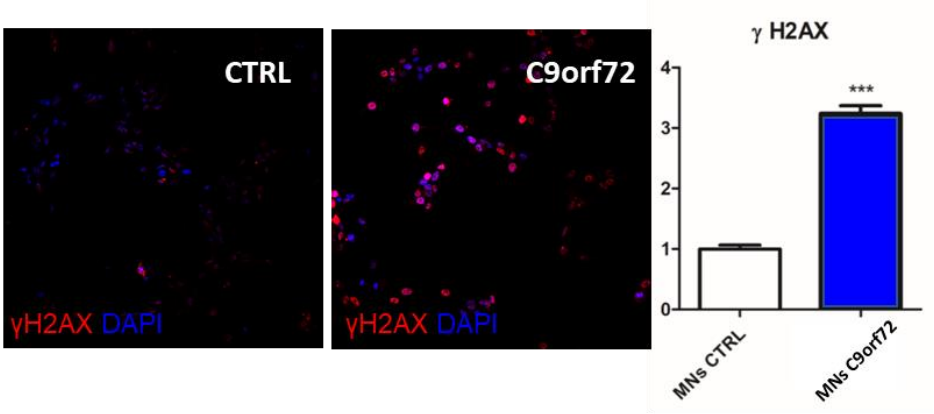

Fig. 4.14. γH2AX expression by immunofluorescence in iPSC-derived MNs. Quantification normalized on control on the right. ****P* < 0.001.

We found this hallmark could be reverted at levels comparable to controls by the treatments with both MOA and MOB in C9orf72-expanded iPSC-derived MNs (Fig. 4.15).

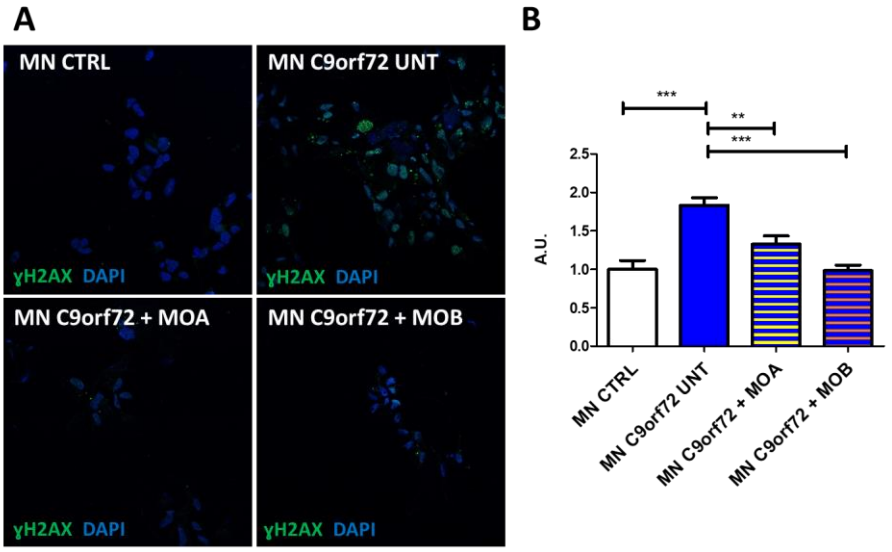

Fig. 4.15. A) Immunofluorescence showing the staining for γH2AX in iPSC-derived MNs. Quantification *P* < 0.01 for *C9orf72* untreated vs MOA-treated, *P* < 0,001 for *C9orf72* vs both untreated and MOB-treated.

The expression of *CDKN1A* and *GADD45a* was measured by qPCR to validate with other markers and a different technique the same result (Fig 4.15, $P < 0.001$ for both genes).

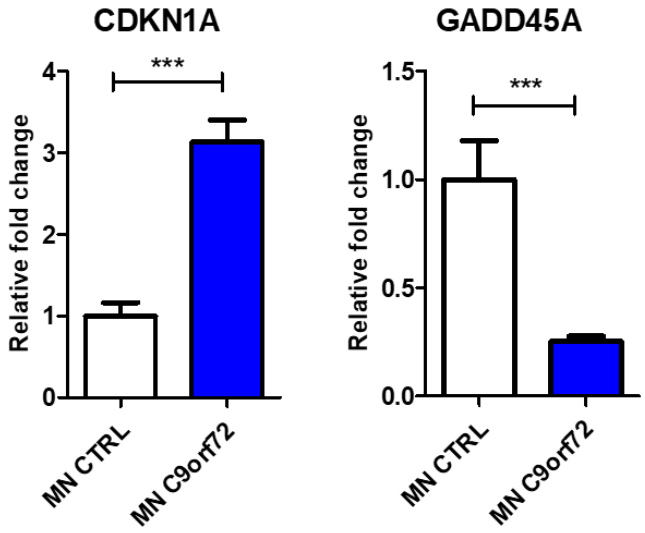

Fig. 4.16. DNA damage markers mRNA expression by qPCR, normalized on control, in iPSC-derived MNs. Student's t-test, *** $P < 0.001$.

Like in iPSCs the mRNA level of *CDKN1A* was increase confirming the activation of the DNA damage response pathway. However, *GADD45a* resulted to be down-regulated in iPSC-derived MNs in C9orf72 genetic background (Fig. 4.16). This could be due to the different pathways active in the two different cell types.

4.2.5. Cytoskeletal regulators alteration in iPSC-derived MNs.

From a previous study from our lab, the expression of hsa-miR-138-5p and hsa-miR-127-3p resulted to be strongly upregulated in *C9orf72* expanded MNs derived from iPSCs (Fig. 4.17, $P < 0.01$ for has-miR-

127-3p, $P < 0.05$ for has-miR-138-5p). The expression of the gene *SEPT7*, targeted by both miRNAs, resulted to be repressed in *C9orf72*-expanded MNs, providing an indirect confirmation of miR-138 and miR-127 overexpression. Interestingly, SEPT7 is involved in organization of the actin cytoskeleton. We also evaluated the expression of two genes of the Stathmin family involved in axonal growth, *STMN1* and *STMN2,* previously shown to be impaired in ALS [12]. Both Stathmin genes resulted to be decreased in expanded *C9orf72* background but *STMN2* was not statistically significantly different due to high heterogeneity of controls (Fig. 4.18, $P < 0.05$ *SEPT7* and *STMN1*).

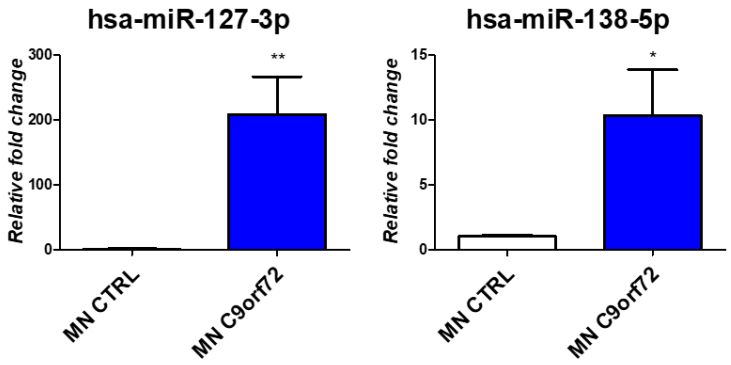

Fig. 4.17. miRNA expression by qPCR in iPSC-derived MNs. $^{**}P < 0.01$ and $^{*}P < 0.05$ for has-miR-127-3p and has-miR-138-5p respectively.

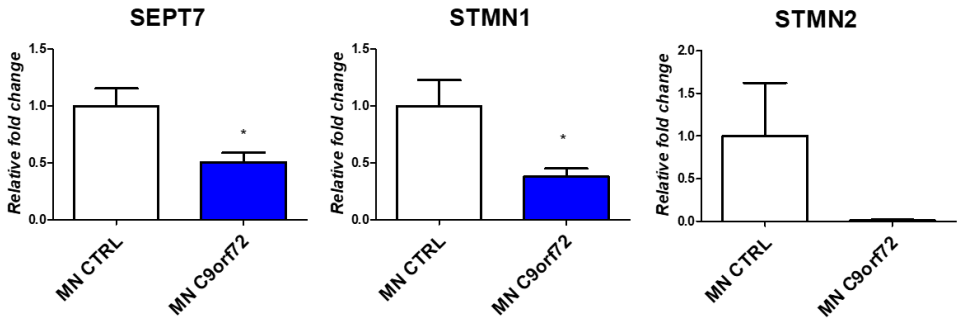

Fig. 4.18. Cytoskeletal regulators expression by qPCR, normalized on control, in iPSC-derived MNs. *$P < 0.05$ for *SEPT7* and *STMN1*.

4.2.6. Axonal lengths in iPSC-derived MNs.

Since the expression data highlighted an alteration of cytoskeletal regulation, a further investigation of cytoskeletal abnormalities was performed. Using Incucyte automated tracking analysis MNs differentiated from *C9orf72*-expanded and control iPSCs have been live imaged for a week and their axonal lengths were measured. It resulted that expansion carrying MNs had shorter axons (Fig. 4.19).

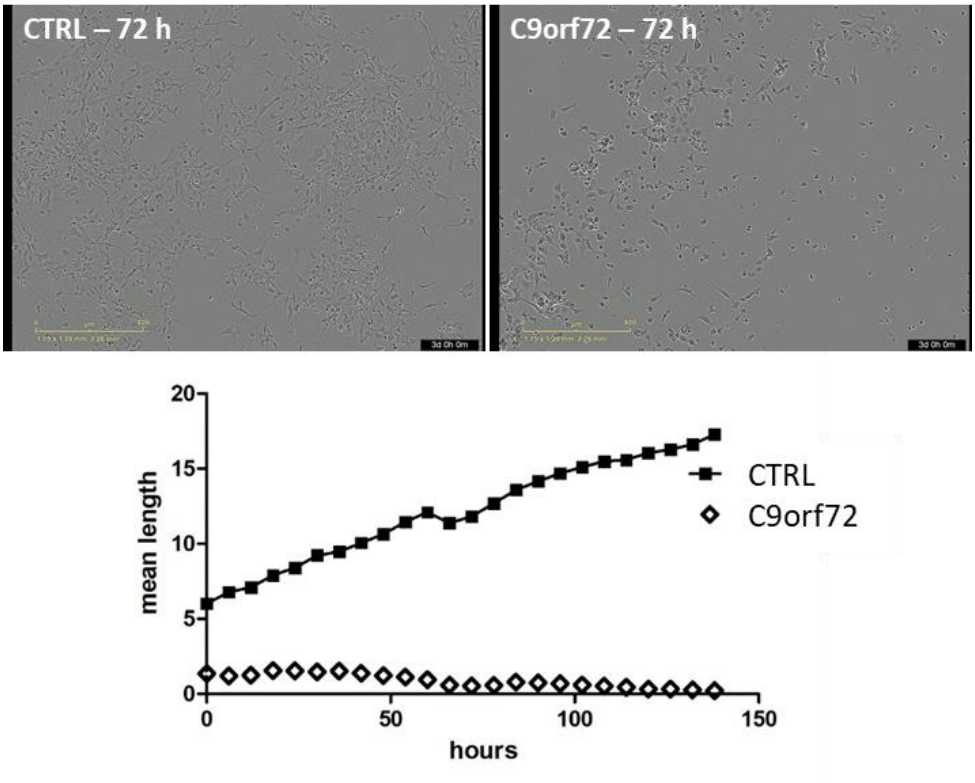

Fig. 4.19 Brightfield representative frames at 72 hours of time-lapse live imaging of iPSC-derived MNs (upper) and Incucyte automated axonal length measurements (lower).

Axonal length was also evaluated after staining with Neurofilament heavy chain (SMI32). Axons have been measured analyzing the images with NeuronJ plugin.

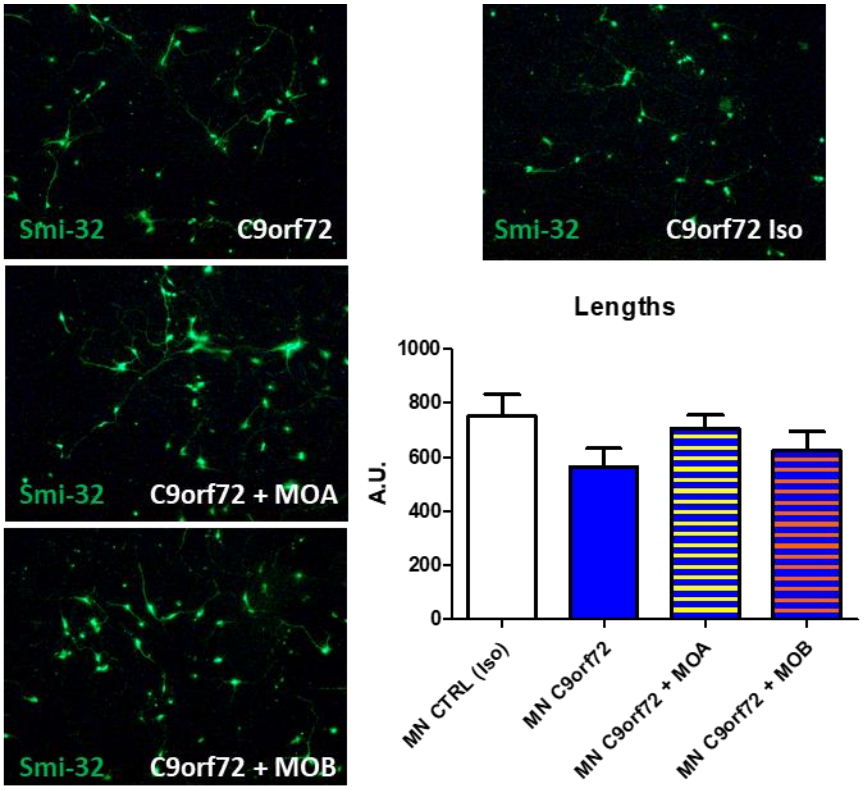

Fig. 4.20. Immunofluorescence images of iPSC-derived MNs stained for SMI32 (green) and axonal lengths quantification.

Comparing MNs deriving from diseased and isogenic corrected iPSC lines no statistically significant evidences of difference in length was detectable between *C9orf72* background and controls, anyway a trend seemed to appear showing shorter axons in *C9orf72* lines and with MOs-treated lines rising toward control levels (Fig. 4.20).

4.2.7. Global gene expression profiling alteration in ALS iPSC-derived MNs and after MO treatment.

The global gene expression has been investigated in iPSC-derived MNs with the Nanostring nCounter technology with the same Neuropathology Panel previously described for iPSCs. The comparison of *C9orf72* MNs with the isogenic corrected counterpart showed an upregulation of genes involved in Inflammatory response, Immune cell trafficking, Cell-to-cell signaling and interaction, Cellular Growth and Proliferation, and Cellular Development. Conversely a group of sub-pathways related to Neurological Disease seemed to be repressed.

Treatment with MOB could mildly recover the upregulation for some subpathways of the categories indicated, most interestingly data indicated the recovery in the subpathways belonging to Neurological Disease category and the majority under Inflammatory response. Also, the category of Immune cell trafficking, which was upregulated in C9orf72-expanded MNs in respect with healthy ones, recovered after MOB treatment, showing the downregulation of many genes involved in this category (Fig. 4.21)

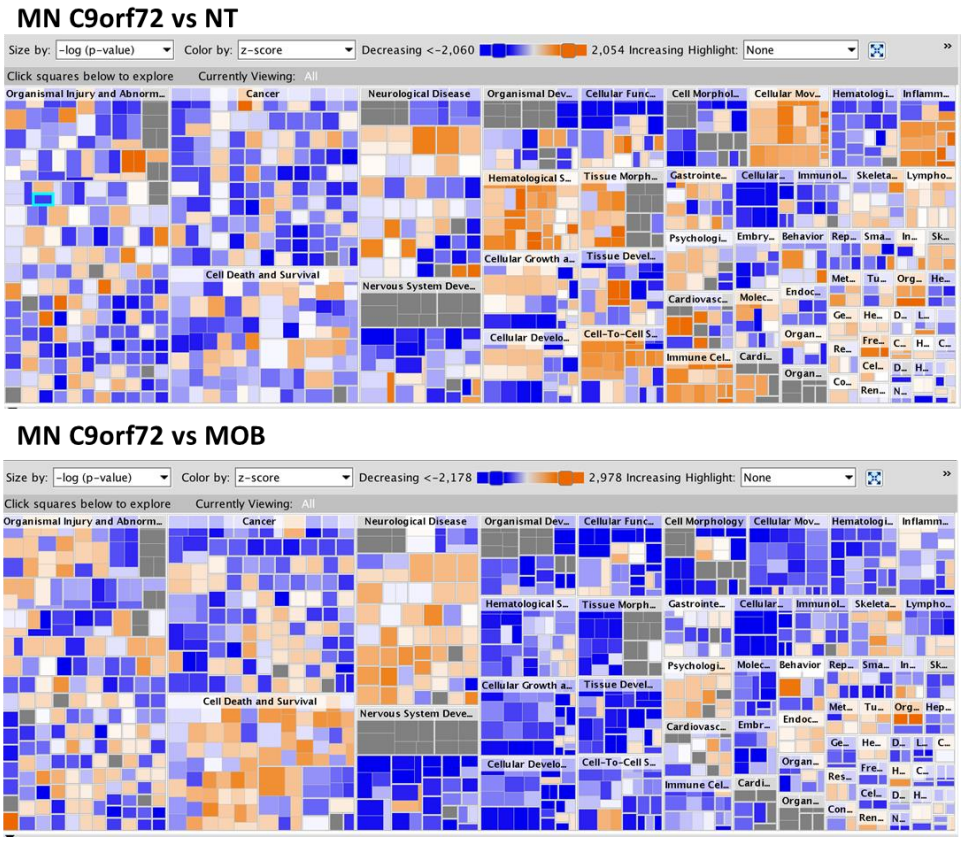

Fig 4.20. Deregulated pathways in C9orf72 vs NT (upper) and C9orf72 vs MOB-treated iPSCs (lower) iPSC-derived MNs.

4.3. Organoid model for C9orf72-ALS.

4.3.1. Production of Spinal cord-like Organoids.

As a more advanced disease model, we generate CNS organoids, Brain and Spinal cord. We have been able to produce a first batch pairing *C9orf72*-expanded iPSC line with iPSC CTRL_1 line and characterize it. The protocol used was the one from Lancaster et al. [58] for the Whole Brain and a modified protocol for Spinal cord.

Organoids were cultured in spinning flask bioreactors and collected for characterization at timepoints one, two and three months. For immunofluorescence staining, organoids were fixed in PFA, embedded in gelation/sucrose solution and stocked as frozen samples until the cryosectioning. Sliced from organoids were then characterized by immunofluorescence.

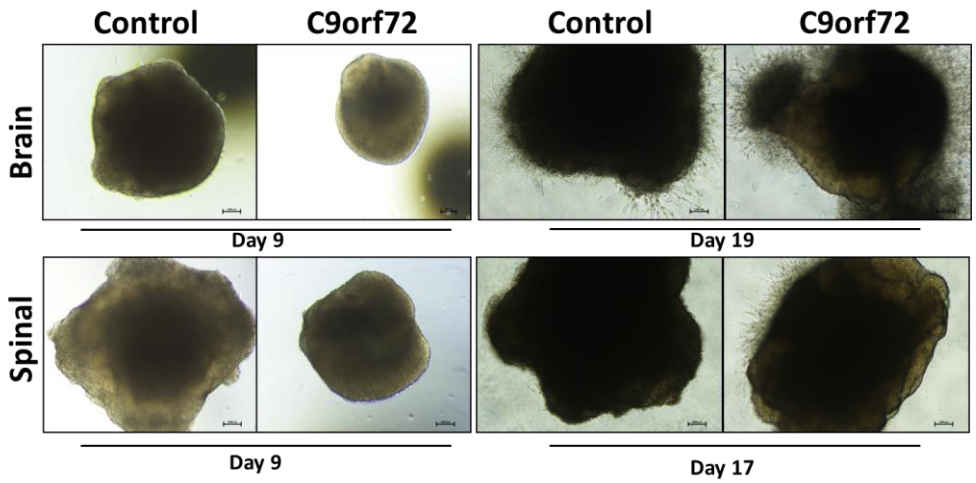

Fig. 4.22. Representative brightfield images of brain and spinal cord organoids collected before starting the growth in spinning flask.

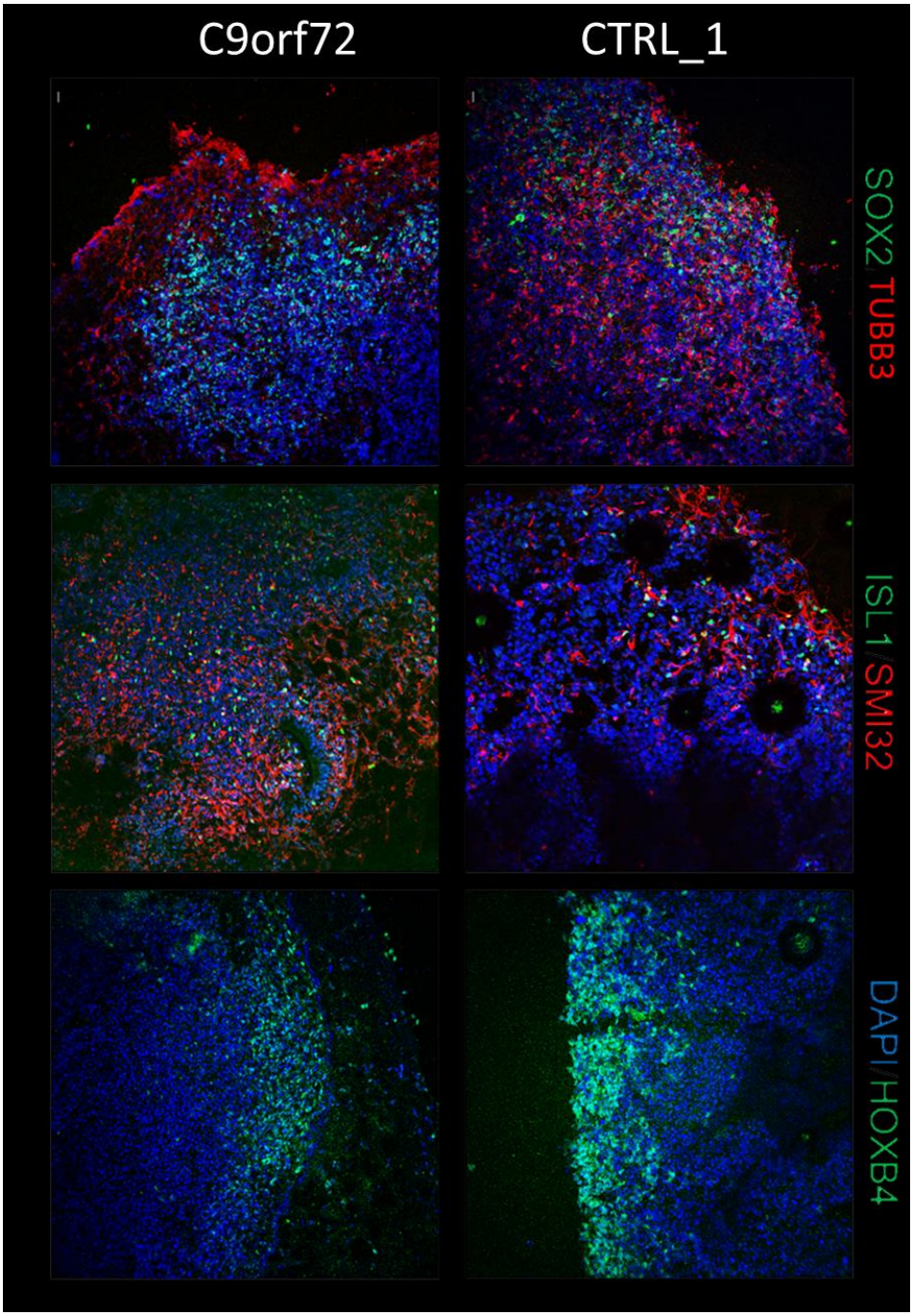
C9orf72
CTRL_1
SOX2 TUBB3
ISL1/SMI32
DAPI/HOXB4

Fig. 4.23. Spinal cord-like organoid model validation. Immunofluorescence images of organoids showing the expression of SOX2 in green and TUBB3 in red from staminal progenitors and more differentiated neurons respectively (day 98). Expression of characteristics MN markers Islet1 in green and SMI32 in red (day 56). Expression of HOXB4 in green indicates cells positional identity is at least cervical along the rostro-caudal axis (day 98). Nuclei counterstained with DAPI in blue.

The presence of SOX2-positive neural progenitors and TUBB3-positive more committed cells were revealed by immunofluorescence (Fig. 4.23). The expression of the spinal cord MN-specific transcription factor Islet1 and the cytoskeletal protein Neurofilament-heavy chain (SMI32) analysed by immunofluorescence showed the commitment toward spinal MN phenotype (Fig. 4.23). Additionally, the staining with antibody against HOXB4 indicated the acquisition of cervical positional identity of some of the cells pinpointing that the phenotype of our MN is not cortical (Fig. 4.23).

4.3.2. Modelling C9orf72-ALS with Organoids.

The first characterization of disease related phenotype performed on the organoids was an exploratory quantification of DPR with the ELISA-based method. Results are preliminary and the preparation of more replicates is ongoing.

The data collected showed that *C9orf72*-expanded organoids are accumulating more DPR than control ones.

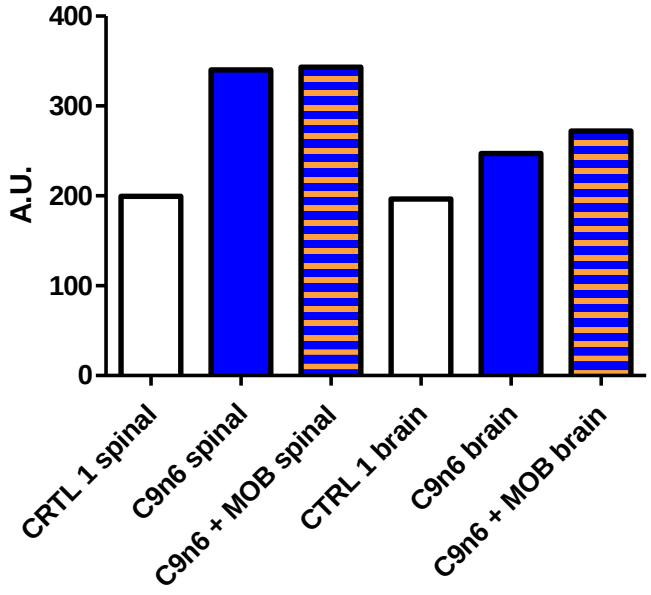

Fig. 4.24. ELISA-based DPR accumulation in organoids.

MOB treatment did not decrease DPR accumulation in *C9orf72*-expanded organoids, both Brain and Spinal Cord. Further analysis is needed since the treatment with MO have been set on MNs, thus switching to a different model the treatment needs to be optimized (Fig. 4.24).

4.3.3. MN genes expression in organoids.

We checked the expression of MN genes in wild-type, *C9orf72*-expanded and *C9orf72* MOB-treated spinal cord organoids.

MN genes *ChAT* and *OLIG2* expressions were measured by real-time qPCR in diseased and healthy spinal cord organoids to evaluate any alteration in MN commitment. The expression of both genes resulted

lower in *C9orf72* organoids in respect with controls with MOB treatment rescuing its level (Fig. 4.25)

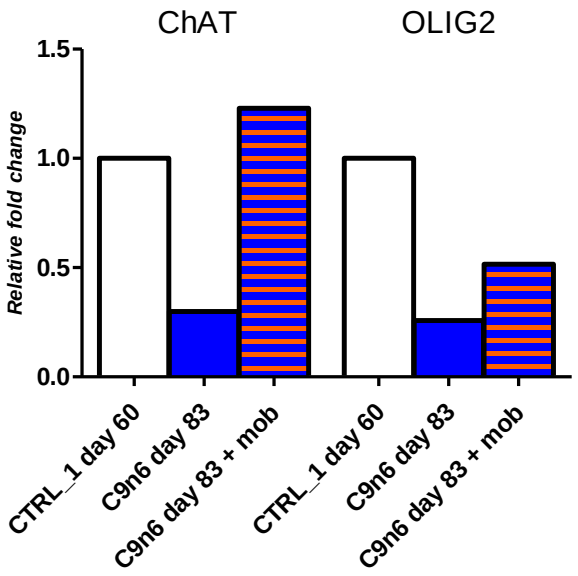

Fig. 4.25. *ChAT* and *OLIG2* expression by qPCR, normalized on control, in organoids and after MOB treatment.

4.3.4. Cytoskeletal regulators alteration in the organoid model.

The alteration of *SEPT7*, *STMN1* and *STMN2* found in iPSC-derived MNs have been investigated in the organoid model to evaluated if they were consistent across these models.

Indeed, mRNA levels of *SEPT7* and *STMN1* were lower in *C9orf72*-expanded organoids as compared with control ones while *STMN2* showed the opposite situation (Fig. 4.26). This result showed that the alteration of these genes can be replicated in both models. Treatment with MOB could rescue the downregulation of *SEPT7* and *STMN1* consistently with iPSC-derived MNs. On the other end *STMN2*

seemed to increase even further in *C9orf72* MOB-treated organoids (Fig. 4.26).

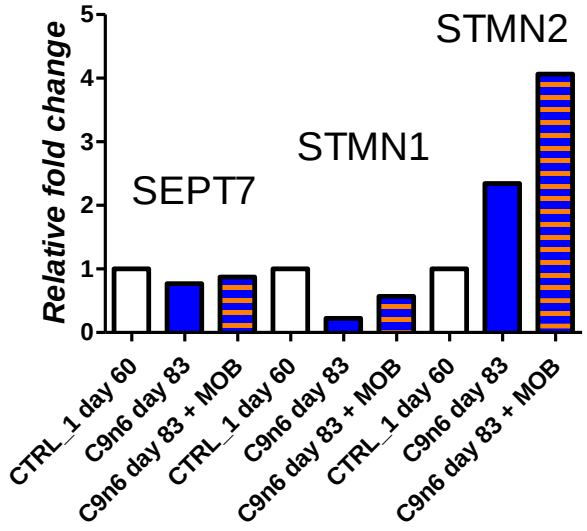

Fig. 4.26. Cytoskeletal regulators expression in organoids by real-time qPCR, normalized on control.

4.3.5. TDP43 translocation.

Another characteristic pathological hallmark of the *C9orf72*-related ALS is the aberrant translocation of TDP43 from nucleus to cytosol. Immunostaining for TDP43 showed clearly cytoplasmic signal for this protein in *C9orf72* organoids when dissociated and plated on coverslips (Fig. 4.27). Interestingly, we could not observe this hallmark in the iPSC-derived MNs (data not shown).

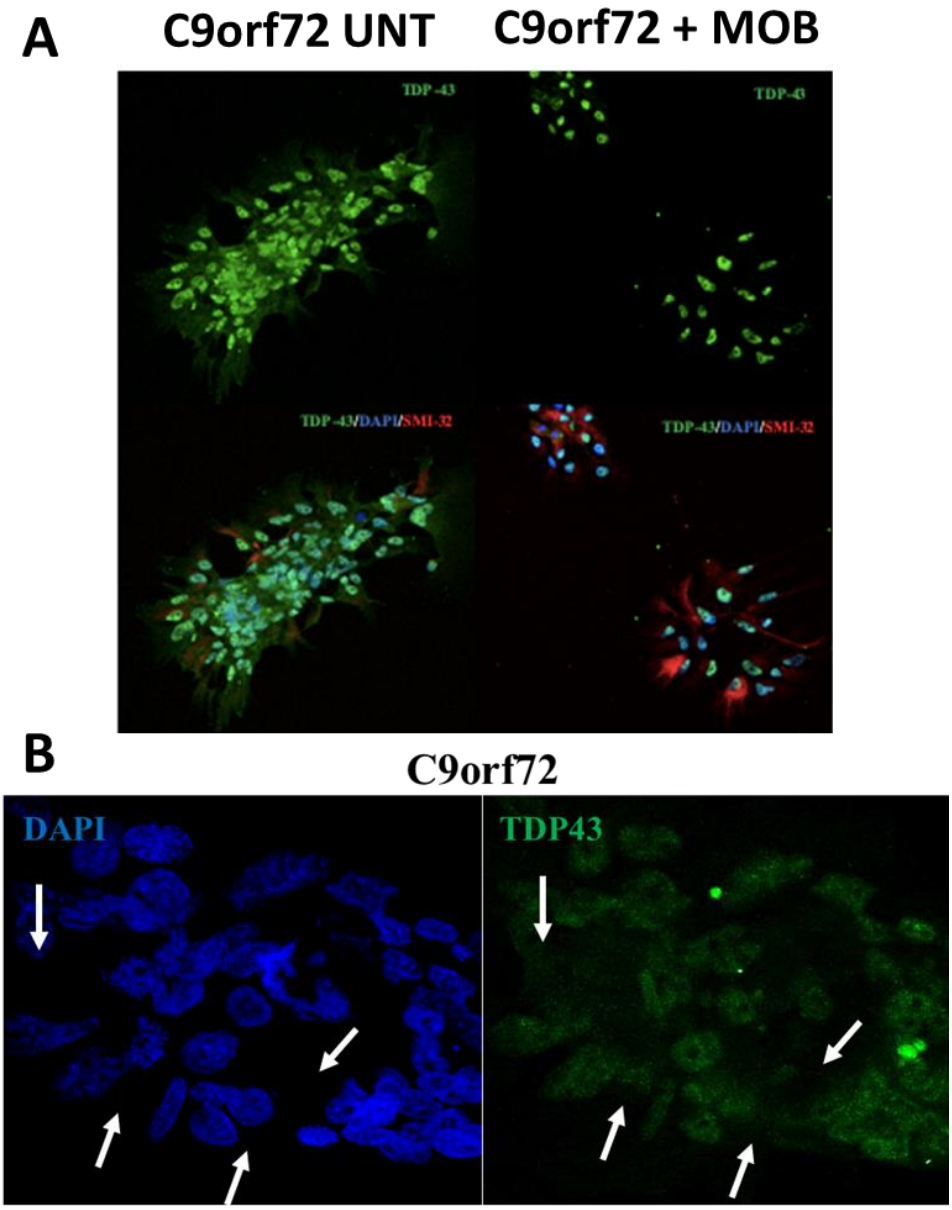

Fig. 4.27. Immunofluorescence of *C9orf72*-expanded dissociated organoids. A) *C9orf72* UNT vs *C9orf72* MOB-treated. Staining for TDP43 (green), SMI32 (red) and DAPI (blue). B) Closer view of nuclei of *C9orf72*-expanded cells. Staining for TDP43 (green) and DAPI (blue), TDP43 mislocalization (white arrow).

5. DISCUSSION.

Amyotrophic lateral sclerosis (ALS) is a fatal neurological disorder characterized by progressive degeneration of motor neurons (MNs) in the cerebral cortex (upper MNs), brain stem and spinal cord (lower MNs). The disease starts in adult life, and the progressive paralysis is typically fatal within a few years, usually due to respiratory failure. ALS is due to mechanisms that are largely unknown. Understanding these events is crucial for developing therapeutics because of the lack of effective treatment for ALS. The absence of reliable preclinical models hampers the progress in the research of its pathogenesis and into the development of rational therapeutic strategies. Thus, there is an urgent need for meaningful progress in this field.

The *C9orf72* is the most frequent ALS causative gene, accounting for the majority of the familiar forms with 40% of cases [15], but it is also related to the 7% of the sporadic forms [16]. The *C9orf72* ALS mutation is an expansion of repeats in a hexanucleotidic non coding sequence. The expanded allele produces RNA foci and DPR, but the mechanism of toxicity is still not clearly understood. Mechanisms proposed cover a wide range of possibilities. On one hand loss of function hypothesis is proposed, the lower level of C9orf72 due to haploinsufficiency cannot fully cover its physiological function [66]. On the other hand, gain of function hypothesis speculates on the toxic mechanisms caused by products of aberrant *C9orf72* transcription (RNA foci) and RAN translation (DPR), like RNA foci sequestration of RNA-binding proteins preventing them to fulfill their function [48] and DPR-mediated increase of oxidative stress and DNA damage [60,67].

To date, a resolutive therapy is not available for ALS and only two drugs, which can only modestly slow the disease progression by few months, received FDA approval [4]. The investigation of *C9orf72*-related ALS is hindered by the lack of a suitable model that fully recapitulates hallmarks of the disease. Animal models of ALS do not fully recapitulate the pathological features found in human, and 2D human-derived cellular models present only some of them. The proper cell type targeted by the disease is of difficult access and the use of easily accessible cells such as fibroblasts obtained from skin biopsy help researchers in finding some clues about the pathology, but models that reflect the Central Nervous System are needed and lacking. In this context, iPSCs can be an important tool. Like fibroblasts, iPSCs carry the same genetic background of the patient, but they can also be differentiated into the target cell type of the disease. This approach has been already used for many neurodegenerative diseases, including ALS [46–48,50,67,68].

Based on this context, our project aimed at 1) the development of a model of *C9orf72* ALS using patient-specific iPSCs differentiated into MNs in 2D and 3D *in vitro* systems, 2) identify known (RNA foci/DPR accumulation) and novel (nuclear pathology/RNA perturbation) pathogenetic events, and 3) develop a novel therapeutic strategy based on ASO with morpholino (MO) chemistry against *C9orf72* expansion. The transversal analysis of these three models allowed us to take advantages of their different features. In the case of iPSCs we could benefit from the relative readiness in establishing the model, their ability to be kept in culture for longer period in respect with

primary cell lines and their ability to recapitulate the basic molecular characteristics of the C9orf72 ALS, as RNA foci and DPR accumulation. Moving to the iPSC-derived MNs we can analyse MN-specific features and to study directly the ALS target cell type which is normally inaccessible. Organoids, allowed us to better model the disease since they can reproduce more in detail the conditions present inside the CNS in respect with the other models, this allows cells to reach a more mature differentiative states and it recreates the majority of the cell to cell interactions present inside the brain.

It is worth to note that coming directly from the patients iPSCs possess the same genetic background of the individual. This allows researcher to take into consideration the presence of eventual modifier genes and offers the advantages of a human model in respect with the animal ones. Moreover, existing animal model of ALS do not recapitulate the phenotype properly and so model like the one used in this study should be preferred.

From this point of view it is important to critically consider every model in the prospective of what it can model better.

As first step, we characterized the iPSCs reprogrammed from ALS patients' skin biopsies. Their self-renewal properties allow them to be expanded in culture for longer period of time than primary cell lines, moreover they can be differentiated into the target tissue of the disease, but they also can be promptly used as model for drug screening and toxicity studies.

Deriving directly from patients, iPSCs bear the same identical genetic background of the affected individual, this also allowed to recreate eventual disease modifier present in the patients genetic backgrounds. iPSCs expressed the bona fide stem cells markers and were pluripotent. In iPSCs we measured the deposition of *C9orf72*-related RNA foci and accumulation of DPR demonstrating that they were significantly increased in the diseased lines with respect to control. This result supports the idea that iPSCs can recapitulate some of the pathological mechanisms of *C9orf72*-ALS and can be used as a disease model.

A downstream effect of the hexanucleotide repeat expansion pathogenic cascade seems to be the induction of DNA damages [60] through several not fully understood mechanisms [67]. We choose a series of DNA damage markers: phosphorylation of H2AX by ATM that is one of the first event occurring after damage sensing [69], BRCA1 accumulation due to its recruitment to DNA damage as a transducer in the DDR cascade [70], increase of expression of *CDKN1A* and *GADD45a* which are involved in the DDR [63]. Interestingly, our iPSC lines showed a high accumulation of DNA damage as validated by immunofluorescence of DNA damage markers γH2AX and BRCA1 and an increased gene expression of *CDKN1A* and *GADD45a*. These results proved the involvement of DNA damage response in the pathology, due to DPR downstream mechanisms [67] or *C9orf72*-related R-loops formation [71,72]. The deregulation of this pathway may be responsible for the higher level of R-loops.

We investigated whether these alterations can be reverted by an ASO MO treatment as a proof of principle for a therapeutic approach. Use of ASO targeting *C9orf72* to reduce the repeat-containing transcripts in order to decrease gain of function toxicity is a promising therapeutic strategy. Several studies have already shown the efficacy of ASOs in reducing pathological phenotype *in vitro* and *in vivo C9orf72* ALS models [56,68,73]. ASO with phosphorothioate chemistry are under investigation in a phase 1 clinical trial (NCT04288856) in C9orf72 patients, given the promising preclinical results. MOs backbone is built upon phosphorothioate lacking the phosphodiester moiety which is the substrate of endogenous nucleases. This results in MOs longer half-life in respect with ASO thus making it possible to reduce the number of treatments needed in clinical setting. Moreover, MOs are better tolerated by the host since they do not induce innate immune response like ASOs [74].

In our project, we designed two novel different ASOs with MO chemistry to reduce the level of aberrant mRNA accumulation: MOA was designed against the ATG and thus it should reduce the translation of the *C9orf72* mRNA. A possible minimal drawback in this strategy is that this molecule can downregulate the translation of all the transcripts, and thus it might exacerbate the pathological mechanism related to protein loss of function, if relevant in the pathogenesis. Instead, MOB is designed on the expansion to block the aggregation of the aberrant transcripts without affecting the overall level of *C9orf72*-encoding mRNAs, and thus it seems more suitable for therapeutic purposes.

In our experiments, both MOs reduced the accumulation of RNA foci in C9orf72 cells. Also, DPR level was reduced by our treatment even if MOA was less efficient than MOB. Treatment of iPSCs with both MOA and B were able to rescue the gene expression alteration of *CDKN1A* and *GADD45a* and also p21 was reduced to level comparable to controls. *GADD45a* works downstream of p53 to regulate heterochromatic status of short telomeres, it physically binds to PCNA and p21 protein to induce cell cycle arrest, it improves accessibility of DDR agents to telomeric chromatin and this may transduce the DDR signal to downstream effectors which are responsible for senescence and or apoptosis [75]. SIRT1, as DDR activation marker, is found to be downregulated by MOs treatments in *C9orf72* expanded iPSCs in respect with untreated and wild-type. Being SIRT1 a regulator of the DDR we can speculate that it is more important in the phase in which DNA damage is induced. We hypotize that in chronic DNA damage presence it is no longer extensively needed since the DDR machinery has already reached an active steady state. Conversely, MOs treatment likely turned off the DNA damage and the DDR machinery starts to be dismantled with subsequent disappearance of the stimuli which sustain SIRT1 production. This could be proven by analyzing for a longer time *SIRT1* expression upon MOs treatment.

The expression of all the *C9orf72* isoforms were found downregulated after both MOs treatment, this finding is not expected since MOs should not interfere with the mRNA target levels but only with its ability to be transcribed. However several experimental evidences show

decreased level of target mRNAs, suggesting that MOs could also affect transcription in some way, inducing mRNA degradation. Quantification of C9orf72 isoforms expression is still challenging and in literature different discordant options are presents [23,24,56], Moreover, in quantification of the different *C9orf72* transcripts by real-time PCR with SYBR green chemistry is not well defined. Primer flanking the expansion cannot amplify transcripts produced by the expanded allele due to the expansion-containing intron retention. A clear explanation for this phenomenon in our model is still lacking and further investigation is needed.

RAN translation seems to be induced upon cellular and genotoxic stress [33], so it is reasonable to argue that our MO strategy is active on stopping a feedback loop in which DPR induce DNA damage and vice versa, as proved by the nuclear stress markers normalization. The toxic effect of DPR on nuclear level has been described also in other experimental settings. In a paper by Lopez-Gonzalez et al. [67] researchers found that GR-DPR bound to mitochondrial ribosomal proteins compromising mitochondrial function thus inducing DNA damage by increasing oxidative stress. Moreover, they found long chain of $(GR)_{80}$-DPR to interact with nuclear protein such as Laminin B receptor and RNA-binding protein like *MATRIN3*. Together with a progressive deterioration of nuclear pore functionality authors suggested a direct nuclear involvement in the accumulation of DNA damage. The specific mechanism by which these interactions could hinder DNA integrity is still not completely clear. We do not have new mechanistic evidence but MOs treatment reduced both DPR, p21

levels and *CDKN1A* and *GADD45a* DNA damage markers expression in our model, suggesting overall a protective effect of MO on nuclear stability.

We investigated also global gene expression alteration with the Nanostring nCounter technology. Previous effort to analyse gene expression alteration in *C9orf72*-expanded samples have been already done [48,56,76] but the focus was not on iPSCs. The majority of transcriptome dysregulation are likely due to TDP43-related pathology rather than *C9orf72* mutation per se [77] and they were mild gene expression alteration mostly targeting pathway involved in vesicles trafficking [77] and RNA metabolisms and alteration [50]. The vast majority of the deregulated genes that we found in *C9orf72*-expanded lines were involved in the regulation of cell proliferation, but also many downregulated genes belonged to the pathway Nervous System Development. It is not clear why the expansion in C9orf72 causes alteration in genes involved in cell proliferation, this effect may be an artifact due to the specific cell type. Indeed, iPSCs, which underwent the whole reprogramming process, are still compared with their healthy counterparts which went through the same steps. Further investigations are needed but iPSCs must be carefully evaluated in line with their ability to model pathological features they are more able to reproduce RNA foci and DPR. As proven by the downregulation of genes involved in Nervous System Development , defects in neurodevelopmental aspects can be relevant to the subsequent neurodegenerative disease by causing in iPSCs a lack priming toward the neural phenotype, but this hypothesis has to be experimentally

assessed. The same analysis comparing untreated with MOB-treated iPSCs showed a rescue, almost completely reverting the expression deregulation. This proved that removing the first cause of the disease all the other molecular features can return to their basal state.

Unfortunately, iPSCs cannot fully recapitulate pathological features typical of MNs, which are the main cell target in the *C9orf72*-ALS, like neurodegeneration or electrophysiological alterations. However, taken together, our findings suggest that iPSCs can model the canonical as well as recently discovered pathological hallmarks, and they can be used to screen drugs targeting the hallmarks already present in this model thanks to the relatively short time required in culture experiments in respect with more advanced models like iPSC-derived MNs and organoids.

Moving forward, we characterized iPSC-derived MNs. Differentiating iPSCs from *C9orf72*-expanded affected individuals we can investigate in a dish the pathological events present in the patients. The first step was to probe this model for the presence of RNA foci and DPR accumulation. Our results showed that diseased iPSC-derived MNs had increased RNA foci and DPR accumulation and MO treatment, with both MOA and MOB was able to reduce them.

DNA damage induction has been analysed showing that, like iPSCs, also *C9orf72* iPSC-derived MNs had higher phosphorylation level of γH2AX. The gene *CDKN1A* is upregulated in *C9orf72*-expanded MNs in respect with controls. Expression of *GADD45a* is reduced in *C9orf72*-expanded lines, suggesting different regulation of the DNA

damage response [75] in MNs compared with iPSCs. This could be due to differences in DDR pathways active in the different cell types, GADD45a is known to generate a more permissive chromatin states in sub-telomeric regions to regulate DDR in intestinal adult stem cells [75], a mechanism that could be active in the opposite direction in MNs where to avoid access to telomeric region of the repairing machinery GADD45a is downregulated. This could avoid possible damage to telomeres which MNs are not able to properly repair or MNs may downregulate it in order to avoid apoptosis as ultimate response to DDR activation. GADD45a is involved in epigenetic regulation also, so a mechanism of DNA repair regulated by epigenetic modification could be the culprit of this downregulation [78]. Moreover, iPSCs are actively proliferating cells, so upon DNA damage it should be important for them to overexpress genes that can induce cell cycle arrest, while for terminally differentiated cell which do not undergo proliferation, like MNs, the opposite may be beneficial. For sure further investigation is needed.

Thanks to unpublished result from our laboratory, we knew that has-miR-127-3p and has-miR-138-5p are upregulated in *C9orf72*-expanded iPSC-derived MNs so we focused on their target gene *SEPT7* which is a cytoskeleton regulator with important functions in the nervous system. *STMN2*, another cytoskeletal regulator, was found deregulated in ALS models [11,12]. In their papers both groups showed that alteration of *STMN2* gene can hinder neurite outgrowth and axonal regeneration. In line with this evidence, we investigated the alteration of *SEPT7*, *STMN1* and *STMN2* as gene involved in the

cytoskeletal function, which could be more important in neurons then in other cell types.

Real time qPCR data proved *SEPT7*, *STMN1* and STMN2 to be downregulated in *C9orf72*-expanded MNs. Therefore, we investigated more in depth the cytoskeletal alteration by measuring axonal lengths. This parameter turned out to be variable among cell lines so we decided to perform this analysis on a pair of C9orf72-expanded and its isogenic corrected control. Our analysis did not find a statistically significant difference between *C9orf72*-expanded and the isogenic corrected line, but a trend seemed to emerge. Corrected iPSC-derived MNs presented axon longer than *C9orf72* ones and MO treatments increased their axonal length. Alteration of expression of *SEPT7*, *STMN1* and STMN2 in *C9orf72* MNs could be related to an alteration of cytoskeletal function rather than the axonal length itself [79], including deregulation of transport of intracellular loads or cell response to mechanical stress [80,81]. Further investigations are needed to decipher the role of cytoskeletal impairment in *C9orf72* pathogenesis.

Global gene expression analysis on iPSC-derived MNs showed an upregulation of genes involved in inflammation, cell to cell communication and cellular growth and proliferation while genes involved in nervous system-related function were repressed. This result is interesting since it suggests an activation of immune response by MNs themselves, as already proven in the framework of ALS [82,83]. For example the production and secretion of interleukines by

MNs could induce the migration of immune cells toward the CNS, contributing to inflammation-induced damages present in the pathology. Some of these pathways are involved the interplay between different cell types other than MNs, confirming that ALS pathology is also connected to non-neuronal cell type and it partially involves non cell-autonomous mechanisms. In this regard, the implementation of the organoid model can further improve our knowledge about the deregulation of these pathways. Interestingly, genes involved in cellular growth and proliferation could pinpoint an alteration similar to that found in Spinal Muscular Atrophy [84]. Authors found that SMA MNs overexpressed genes involved in cell cycle regulation and in re-entry in the cell cycle as suggested by their expression of Ki67, an active proliferating cell marker. It is known from the literature that the activation of DDR in neurons can induce apoptosis by forcing neurons to re-entry in the cell cycle [85]. The dysregulation of genes involved in proliferation seems more a consequence of DNA damage induction rather than a cause of distress since the molecular event inducing the damages should arise mechanistically before the deregulation of gene expression. The pathway of neurons toward apoptosis seems to be multiple, however the activation of cell cycle components should definitively play a role, therefore the chemical inhibition of these components [86] could be an interesting approach to block the deleterious process ongoing in the diseased cell. From these evidences resulted that, when highly organized, non-proliferating cells, like neurons, try to re-enter in the cell cycle the outcome can be catastrophic for the cell itself.

In the model of iPSC-derived MNs cells are relatively “young”, since they originate from reprogrammed cells. Indeed, they have acquired their cellular phenotype recently in the experimental timeline and, even when kept in long term culture, they seem to be able to acquire only less mature characteristic than *in vivo* adult MNs. This could be the cause of their apparent failure to reproduce some disease hallmarks of a late onset disease as ALS. One of the most interesting hallmark which is not easy to reproduce yet is the neurodegeneration itself. Being relatively young iPSC-derived MNs do not degenerate in culture, this is probably due to the impossibility for them to accumulate enough deleterious events to cause actual cell death. The modelling of the aged phenotype is still one of the goals of the research nowadays.

Then, we decided to take advantage of newly established 3D models: the organoids. These are 3D self-organizing structures that reproduce in miniature organ i.e. the brain. They are able to recreate a more physiological environment respect to the 2D cell cultures allowing to reproduce the interactions occurring between different cell types and thus allowing to investigate the disease hallmarks in a more complex environment considering autonomous and non-autonomous cell death.

No attempt to model ALS with CNS organoids has been described in the literature yet and only very few publications covered the differentiation of 3D spinal cord-like structures [87]. The organoid model lacks of the contribution of the immune system but most of the different cell types present in the CNS and involved in the disease

should be present in our model allowing us to better recapitulate non cell-autonomous hallmarks and properties arising from the network formation, only mildly present in in 2D MNs culture.

From the preliminary data collected so far, we found that *C9orf72*-expanded organoids model the pathologic accumulation of DPR. We found that *C9orf72*-expanded cell line gave rise to organoids which accumulated higher level of DPR than controls. However, MOB treatment did not reduce the DPR, likely because the 3D structure reduces the MO penetration. The treatment of organoid with MOB still need optimization, it is possible that some parameters like dosage and time of exposure should be changed from the protocol used for iPSC-derived MNs, since the two model are relatively different.

The analysis of *OLIG2* and *ChAT* genes expression in the organoids model is helpful to evaluate the cellular composition and the relative presence of precursor cells/differentiated neurons, as marked respectively by *OLIG2* and *ChAT*. Remarkably we found that *C9orf72*-expanded organoids had deficit in the expression of *ChAT* and *OLIG2* in respect to controls, whether this is an actual alteration in neuronal commitment has to be investigated. The treatment with MOB was able to rescue this downregulation.

Another important hallmark present in *C9orf72*-ALS is the mislocalization of TDP43 into the cytosol. This feature is not present in iPSC-derive MNs while it could be recreated into the organoid model. This may prove that TDP43 mislocalization is promoted by the interaction among cells or that organoids are able to mimic better the

normal environment present in the CNS than 2D models. Indeed, culturing organoids allows to sustain the differentiation of MNs for longer time and in a more physiological way than a 2D model, so this could be the key to obtain more differentiated mature cells [88,89] and closer to real pathophysiology of the disease. However, no clear signs of loss of MNs were evident in our organoids, suggesting that a longer maturation is needed to accumulate deleterious events in the cells which compose the organoid and thus observe pathological aging-related features in this model.

As future studies we want to confirm our results and refined global gene expression analysis is going to point put which pathways are deregulated in the disease. Hopefully, this could lead to the discovery of new important therapeutic targets and give us insights on the deregulation of functional hallmarks, like cytoskeletal regulators alteration, already identified.

Being organoids the best model available based on our results, we will further characterization it. For this purpose, more advanced analysis will be helpful, such as omics analysis like single-cell RNA-Seq. This study will be very important to investigate the presence of different cell types and understand their contribution to the pathology of *C9orf72*-ALS. As functional analysis the next step will be the electrophysiological characterization. The multi-electrode array (MEA) is the most promising tool since it allows us to understand electrical activity at the network level, which is one of the features that only organoid model can reproduce.

On the other hand, the *in vivo* validation of our MOs treatment will prove the feasibility and efficacy of this therapeutic approach. Though a satisfactory *C9orf72*-ALS animal model is not present, some molecular features, such as RNA foci and DPR accumulation, are present in some *C9orf72* mouse models [41]. By investigating MOs effect on RNA foci and DPR in these models, as culprit of the downstream pathological alteration, we could prove the efficacy of this kind of approach *in vivo* [90].

Hallmark	Induced Pluripotent Stem Cells	iPSC-derived Motor Neurons	Organoids
Basic validation.	Stem markers: OCT4 and SSEA-4.	MNs markers: TUBB3 and HB9.	SOX2 and TUBB3 markers for progenitors and neurons respectively. MNs markers Islet1 and positional identity marker HOXB4 for spinal protocol.
RNA foci.	Presence of RNA foci in C9orf72 expanded cells.	Presence of RNA foci in C9orf72 expanded cells. MOs treatments (still not significant due).	
DPR accumulation.	Higher DPR levels in C9orf72 expanded cells rescued by MOB (MOA not significant).	Higher lvels in C9orf72 expanded cells. MOs treatments (still not significant due).	Higher DPR levels in C9orf72 expanded cells (still not significant due to numerosity, future studies will increase it). MOs treatment to be optimized.
DNA damage.	Higher levels of BRCA1, pBRCA1 and ɣHA2X in C9orf72 expanded cells. Higher p21	Higher level ofɣHA2X in C9orf72 expanded cells	

	levels in C9orf72 expanded cells rescued by MOs treatments.	rescued by MOs treatments.	
DNA damage gene expression.	Higher CDKN1A and GADD45a in C9orf72 expanded cells rescued by MOs treatments.	Higher level of CDKN1A but lower level of GADD45a in C9orf72 expanded cells.	
Pathways deregulation.	Broad downregulation in C9orf72 expanded cells rescued by MOB.	Downregulation: neurological disease-related pathways. Upregulation: inflammation, cell-to-cell communication and cell-cycle in C9orf72 expanded cells. Rescue by MOB.	
Neuronal cytoskeletal regulators.	Not investigable.	Lower levels of *SEPT7*, *STMN1* and *STMN2* in C9orf72 expanded cells.	Lower levels of *SEPT7*, *STMN1* and *STMN2* in C9orf72 expanded cells rescued by MOB (still not significant due to numerosity, future studies will increase it).

Axonal lengths.	Not investigable.	Not significant but a trend emerges with C9orf72 expanded neurons with shorter axonal lengths than control and MOs treatment increasing them.	
MNs gene expression.	Not investigable.		*OLIG2* and *ChAT* downregulation in C9orf72 expanded cells. Rescued by MOB.
TDP43 translocation.			TDP43 found partially translocate into the cytosol in C9orf72 expanded cells.

Table 1. Hallmarks analysed through the different models investigated.

Overall, we demonstrated that the hallmarks analysis in the iPSC derived 2D and 3D model can be a paradigm to follow the pathological events and test potential therapy. iPSCs and iPSC-derived MNs proved to be suitable in order to model the majority of these features, both canonical and non-canonical ones, and thanks to their relatively lower effort demand they can be exploited in drug testing and discovery. However, the most relevant hallmarks can be recreated

better in the organoid model although this is a very demanding model in terms of time and resources, and it needs further characterization.

The research study we proposed will lead to understand this complex disease and speed up the research for novel therapeutics for ALS patients.

6. CONCLUSIONS.

Research on *C9orf72*-ALS is severely hindered by the lack of proper experimental models able to recapitulate all the molecular features of this complex disease. iPSCs technology is extensively exploited in this field [12,46,47,67,68,91,92]. We aimed at the transversal validation of the three models built upon this technology: iPSCs, iPSC-derived MNs, the cell type affected in ALS, and iPSC-derived organoids that can recapitulate CNS complexity.

All three models showed to be able to recapitulate the canonical hallmarks present in the disease which are RNA foci and DPR. Moreover, we validated the presence of DNA damage and activation of DDR [60,67,93,94] in the *C9orf72*-expanded background in both iPSCs and iPSC-derived MNs. Markers of DNA damage were present in the *C9orf72* background in both iPSCs and iPSC-derived MNs models, even they presented different alteration and mechanisms. Moreover, our proof of principle treatment with MOs could rescue, at least partially, all these pathological markers and the canonical RNA foci and DPR accumulation. This confirms the linkage between

canonical *C9orf72*-related molecular features and the induction of DNA damage. The iPSC-derived MNs model gave us the possibility to investigate the proper cell type targeted by the disease. This is the only available way to probe MN-specific alteration *in vitro* and it allowed us to gain insights in the cytoskeletal regulators deregulation.

Analysis of global gene expression in both iPSCs and iPSC-derived MNs model suggested that many deregulated pathways can contribute to the pathology and that non cell-autonomous mechanism probably are active part of the process and MOB treatment was able to rescue some of these alterations.

We demonstrated that 2D models, iPSCs and iPSC-derived MNs, can be used as a tool to model some ALS pathological hallmarks and for drug discovery. However, they failed to reproduce more complex pathological phenotype such as mislocalization, apoptosis and non-cell autonomous death.

Organoids proved to be a more advance model, by being able to model *C9orf72*-related phenotype which were not present in the iPSCs or iPSC-derived MNs models like TDP43 mislocalization. They can offer the key to recreate the whole specific phenotype of the *C9orf72*-ALS, caused by physiologically and complex conditions present into the brain and spinal cord in vivo, thanks to the presence and connection of different cell types and fully mature phenotypes [88,89].

Preliminary results obtained with CNS organoids are very promising. The further functional characterization of these models could open new venues in the field of *C9orf72*-ALS, it may pave the way for a

comprehensive view of the pathological mechanisms and for the discovery of new therapeutic targets for ALS.

BIBLIOGRAPHY.

[1] G. Logroscino, B.J. Traynor, O. Hardiman, A. Chiò, D. Mitchell, R.J. Swingler, A. Millul, E. Benn, E. Beghi, F. Eurals, Incidence of amyotrophic lateral sclerosis in Europe, J. Neurol. Neurosurg. Psychiatry. 81 (2010) 385–390. https://doi.org/10.1136/jnnp.2009.183525.

[2] I. Štětkářová, E. Ehler, Diagnostics of Amyotrophic Lateral Sclerosis: Up to Date, Diagn. Basel Switz. 11 (2021). https://doi.org/10.3390/diagnostics11020231.

[3] M. Nizzardo, M. Taiana, F. Rizzo, J. Aguila Benitez, J. Nijssen, I. Allodi, V. Melzi, N. Bresolin, G.P. Comi, E. Hedlund, S. Corti, Synaptotagmin 13 is neuroprotective across motor neuron diseases, Acta Neuropathol. (Berl.). 139 (2020) 837–853. https://doi.org/10.1007/s00401-020-02133-x.

[4] O. Hardiman, L.H. van den Berg, Edaravone: a new treatment for ALS on the horizon?, Lancet Neurol. 16 (2017) 490–491. https://doi.org/10.1016/S1474-4422(17)30163-1.

[5] A.S. Andrew, W.G. Bradley, D. Peipert, T. Butt, K. Amoako, E.P. Pioro, R. Tandan, J. Novak, A. Quick, K.D. Pugar, K. Sawlani, B. Katirji, T.A. Hayes, P. Cazzolli, J. Gui, P. Mehta, D.K. Horton, E.W. Stommel, Risk factors for amyotrophic lateral sclerosis: A regional United States case-control study, Muscle Nerve. (2020). https://doi.org/10.1002/mus.27085.

[6] S.J. Merwin, T. Obis, Y. Nunez, D.B. Re, Organophosphate neurotoxicity to the voluntary motor system on the trail of environment-caused amyotrophic lateral sclerosis: the known, the misknown, and the unknown, Arch. Toxicol. 91 (2017) 2939–2952. https://doi.org/10.1007/s00204-016-1926-1.

[7] J.M. Morahan, B. Yu, R.J. Trent, R. Pamphlett, A gene-environment study of the paraoxonase 1 gene and pesticides in amyotrophic lateral sclerosis, Neurotoxicology. 28 (2007) 532–540. https://doi.org/10.1016/j.neuro.2006.11.007.

[8] M. Saeed, N. Siddique, W.Y. Hung, E. Usacheva, E. Liu, R.L. Sufit, S.L. Heller, J.L. Haines, M. Pericak-Vance, T. Siddique, Paraoxonase cluster polymorphisms are associated with sporadic ALS, Neurology. 67 (2006) 771–776. https://doi.org/10.1212/01.wnl.0000227187.52002.88.

[9] D.R. Rosen, T. Siddique, D. Patterson, D.A. Figlewicz, P. Sapp, A. Hentati, D. Donaldson, J. Goto, J.P. O'Regan, H.-X. Deng, Z. Rahmani, A. Krizus, D. McKenna-Yasek, A. Cayabyab, S.M. Gaston, R. Berger, R.E. Tanzi, J.J.

Halperin, B. Herzfeldt, R.V. den Bergh, W.-Y. Hung, T. Bird, G. Deng, D.W. Mulder, C. Smyth, N.G. Laing, E. Soriano, M.A. Pericak–Vance, J. Haines, G.A. Rouleau, J.S. Gusella, H.R. Horvitz, R.H. Brown, Mutations in Cu/Zn superoxide dismutase gene are associated with familial amyotrophic lateral sclerosis, Nature. 362 (1993) 59–62. https://doi.org/10.1038/362059a0.

[10] R.H. Brown, A. Al-Chalabi, Amyotrophic Lateral Sclerosis, Http://Dx.Doi.Org.Pros.Lib.Unimi.It/10.1056/NEJMra1603471. (2017). https://doi.org/10.1056/NEJMra1603471.

[11] J.R. Klim, L.A. Williams, F. Limone, I. Guerra San Juan, B.N. Davis-Dusenbery, D.A. Mordes, A. Burberry, M.J. Steinbaugh, K.K. Gamage, R. Kirchner, R. Moccia, S.H. Cassel, K. Chen, B.J. Wainger, C.J. Woolf, K. Eggan, ALS-implicated protein TDP-43 sustains levels of STMN2, a mediator of motor neuron growth and repair, Nat. Neurosci. 22 (2019) 167–179. https://doi.org/10.1038/s41593-018-0300-4.

[12] Z. Melamed, J. López-Erauskin, M.W. Baughn, O. Zhang, K. Drenner, Y. Sun, F. Freyermuth, M.A. McMahon, M.S. Beccari, J.W. Artates, T. Ohkubo, M. Rodriguez, N. Lin, D. Wu, C.F. Bennett, F. Rigo, S. Da Cruz, J. Ravits, C. Lagier-Tourenne, D.W. Cleveland, Premature polyadenylation-mediated loss of stathmin-2 is a hallmark of TDP-43-dependent neurodegeneration, Nat. Neurosci. 22 (2019) 180–190. https://doi.org/10.1038/s41593-018-0293-z.

[13] M. Neumann, D.M. Sampathu, L.K. Kwong, A.C. Truax, M.C. Micsenyi, T.T. Chou, J. Bruce, T. Schuck, M. Grossman, C.M. Clark, L.F. McCluskey, B.L. Miller, E. Masliah, I.R. Mackenzie, H. Feldman, W. Feiden, H.A. Kretzschmar, J.Q. Trojanowski, V.M.-Y. Lee, Ubiquitinated TDP-43 in Frontotemporal Lobar Degeneration and Amyotrophic Lateral Sclerosis, Science. 314 (2006) 130–133. https://doi.org/10.1126/science.1134108.

[14] E.L. Scotter, H.-J. Chen, C.E. Shaw, TDP-43 Proteinopathy and ALS: Insights into Disease Mechanisms and Therapeutic Targets, Neurotherapeutics. 12 (2015) 352–363. https://doi.org/10.1007/s13311-015-0338-x.

[15] E. Majounie, A.E. Renton, K. Mok, E.G.P. Dopper, A. Waite, S. Rollinson, A. Chiò, G. Restagno, N. Nicolaou, J. Simon-Sanchez, J.C. van Swieten, Y. Abramzon, J.O. Johnson, M. Sendtner, R. Pamphlett, R.W. Orrell, S. Mead, K.C. Sidle, H. Houlden, J.D. Rohrer, K.E. Morrison, H. Pall, K. Talbot, O. Ansorge, Chromosome 9-ALS/FTD Consortium, French research network on FTLD/FTLD/ALS, ITALSGEN Consortium, D.G. Hernandez, S. Arepalli, M. Sabatelli, G. Mora, M. Corbo, F. Giannini, A. Calvo, E. Englund, G. Borghero, G.L. Floris, A.M. Remes, H. Laaksovirta, L. McCluskey, J.Q. Trojanowski, V.M. Van Deerlin, G.D. Schellenberg, M.A. Nalls, V.E. Drory, C.-S. Lu, T.-H. Yeh, H. Ishiura, Y. Takahashi, S. Tsuji, I. Le Ber, A. Brice, C. Drepper, N. Williams, J. Kirby, P. Shaw, J. Hardy, P.J. Tienari, P. Heutink, H.R. Morris, S. Pickering-

Brown, B.J. Traynor, Frequency of the C9orf72 hexanucleotide repeat expansion in patients with amyotrophic lateral sclerosis and frontotemporal dementia: a cross-sectional study, Lancet Neurol. 11 (2012) 323–330. https://doi.org/10.1016/S1474-4422(12)70043-1.
[16] A. Iacoangeli, A. Al Khleifat, A.R. Jones, W. Sproviero, A. Shatunov, S. Opie-Martin, K.E. Morrison, P.J. Shaw, C.E. Shaw, I. Fogh, R.J. Dobson, S.J. Newhouse, A. Al-Chalabi, Alzheimer's Disease Neuroimaging Initiative, C9orf72 intermediate expansions of 24–30 repeats are associated with ALS, Acta Neuropathol. Commun. 7 (2019) 115. https://doi.org/10.1186/s40478-019-0724-4.
[17] S. Xiao, L. MacNair, P. McGoldrick, P.M. McKeever, J.R. McLean, M. Zhang, J. Keith, L. Zinman, E. Rogaeva, J. Robertson, Isoform-specific antibodies reveal distinct subcellular localizations of C9orf72 in amyotrophic lateral sclerosis, Ann. Neurol. 78 (2015) 568–583. https://doi.org/10.1002/ana.24469.
[18] T.P. Levine, R.D. Daniels, A.T. Gatta, L.H. Wong, M.J. Hayes, The product of C9orf72, a gene strongly implicated in neurodegeneration, is structurally related to DENN Rab-GEFs, Bioinforma. Oxf. Engl. 29 (2013) 499–503. https://doi.org/10.1093/bioinformatics/bts725.
[19] D. Zhang, L.M. Iyer, F. He, L. Aravind, Discovery of Novel DENN Proteins: Implications for the Evolution of Eukaryotic Intracellular Membrane Structures and Human Disease, Front. Genet. 3 (2012) 283. https://doi.org/10.3389/fgene.2012.00283.
[20] J. Amick, A. Roczniak-Ferguson, S.M. Ferguson, C9orf72 binds SMCR8, localizes to lysosomes, and regulates mTORC1 signaling, Mol. Biol. Cell. 27 (2016) 3040–3051. https://doi.org/10.1091/mbc.E16-01-0003.
[21] P.M. Sullivan, X. Zhou, A.M. Robins, D.H. Paushter, D. Kim, M.B. Smolka, F. Hu, The ALS/FTLD associated protein C9orf72 associates with SMCR8 and WDR41 to regulate the autophagy-lysosome pathway, Acta Neuropathol. Commun. 4 (2016) 51. https://doi.org/10.1186/s40478-016-0324-5.
[22] O. Hardiman, A. Al-Chalabi, C. Brayne, E. Beghi, L.H. van den Berg, A. Chio, S. Martin, G. Logroscino, J. Rooney, The changing picture of amyotrophic lateral sclerosis: lessons from European registers, J. Neurol. Neurosurg. Psychiatry. 88 (2017) 557–563. https://doi.org/10.1136/jnnp-2016-314495.
[23] M. DeJesus-Hernandez, I.R. Mackenzie, B.F. Boeve, A.L. Boxer, M. Baker, N.J. Rutherford, A.M. Nicholson, N.A. Finch, H. Flynn, J. Adamson, N. Kouri, A. Wojtas, P. Sengdy, G.-Y.R. Hsiung, A. Karydas, W.W. Seeley, K.A. Josephs, G. Coppola, D.H. Geschwind, Z.K. Wszolek, H. Feldman, D.S. Knopman, R.C. Petersen, B.L. Miller, D.W. Dickson, K.B. Boylan, N.R. Graff-Radford, R. Rademakers, Expanded GGGGCC hexanucleotide repeat in noncoding region

of C9ORF72 causes chromosome 9p-linked FTD and ALS, Neuron. 72 (2011) 245–256. https://doi.org/10.1016/j.neuron.2011.09.011.
[24] A.E. Renton, E. Majounie, A. Waite, J. Simón-Sánchez, S. Rollinson, J.R. Gibbs, J.C. Schymick, H. Laaksovirta, J.C. van Swieten, L. Myllykangas, H. Kalimo, A. Paetau, Y. Abramzon, A.M. Remes, A. Kaganovich, S.W. Scholz, J. Duckworth, J. Ding, D.W. Harmer, D.G. Hernandez, J.O. Johnson, K. Mok, M. Ryten, D. Trabzuni, R.J. Guerreiro, R.W. Orrell, J. Neal, A. Murray, J. Pearson, I.E. Jansen, D. Sondervan, H. Seelaar, D. Blake, K. Young, N. Halliwell, J.B. Callister, G. Toulson, A. Richardson, A. Gerhard, J. Snowden, D. Mann, D. Neary, M.A. Nalls, T. Peuralinna, L. Jansson, V.-M. Isoviita, A.-L. Kaivorinne, M. Hölttä-Vuori, E. Ikonen, R. Sulkava, M. Benatar, J. Wuu, A. Chiò, G. Restagno, G. Borghero, M. Sabatelli, ITALSGEN Consortium, D. Heckerman, E. Rogaeva, L. Zinman, J.D. Rothstein, M. Sendtner, C. Drepper, E.E. Eichler, C. Alkan, Z. Abdullaev, S.D. Pack, A. Dutra, E. Pak, J. Hardy, A. Singleton, N.M. Williams, P. Heutink, S. Pickering-Brown, H.R. Morris, P.J. Tienari, B.J. Traynor, A hexanucleotide repeat expansion in C9ORF72 is the cause of chromosome 9p21-linked ALS-FTD, Neuron. 72 (2011) 257–268. https://doi.org/10.1016/j.neuron.2011.09.010.
[25] N.J. Rutherford, M.G. Heckman, M. Dejesus-Hernandez, M.C. Baker, A.I. Soto-Ortolaza, S. Rayaprolu, H. Stewart, E. Finger, K. Volkening, W.W. Seeley, K.J. Hatanpaa, C. Lomen-Hoerth, A. Kertesz, E.H. Bigio, C. Lippa, D.S. Knopman, H.A. Kretzschmar, M. Neumann, R.J. Caselli, C.L. White, I.R. Mackenzie, R.C. Petersen, M.J. Strong, B.L. Miller, B.F. Boeve, R.J. Uitti, K.B. Boylan, Z.K. Wszolek, N.R. Graff-Radford, D.W. Dickson, O.A. Ross, R. Rademakers, Length of normal alleles of C9ORF72 GGGGCC repeat do not influence disease phenotype, Neurobiol. Aging. 33 (2012) 2950.e5–7. https://doi.org/10.1016/j.neurobiolaging.2012.07.005.
[26] I.O.C. Woollacott, S. Mead, The C9ORF72 expansion mutation: gene structure, phenotypic and diagnostic issues, Acta Neuropathol. (Berl.). 127 (2014) 319–332. https://doi.org/10.1007/s00401-014-1253-7.
[27] P. Fratta, S. Mizielinska, A.J. Nicoll, M. Zloh, E.M.C. Fisher, G. Parkinson, A.M. Isaacs, C9orf72 hexanucleotide repeat associated with amyotrophic lateral sclerosis and frontotemporal dementia forms RNA G-quadruplexes, Sci. Rep. 2 (2012) 1016. https://doi.org/10.1038/srep01016.
[28] K. Reddy, B. Zamiri, S.Y.R. Stanley, R.B. Macgregor, C.E. Pearson, The disease-associated r(GGGGCC)n repeat from the C9orf72 gene forms tract length-dependent uni- and multimolecular RNA G-quadruplex structures, J. Biol. Chem. 288 (2013) 9860–9866. https://doi.org/10.1074/jbc.C113.452532.

[29] E.G. Conlon, L. Lu, A. Sharma, T. Yamazaki, T. Tang, N.A. Shneider, J.L. Manley, The C9ORF72 GGGGCC expansion forms RNA G-quadruplex inclusions and sequesters hnRNP H to disrupt splicing in ALS brains, ELife. 5 (2016). https://doi.org/10.7554/eLife.17820.
[30] J. Sollier, K.A. Cimprich, Breaking bad: R-loops and genome integrity, Trends Cell Biol. 25 (2015) 514–522. https://doi.org/10.1016/j.tcb.2015.05.003.
[31] P.A. Ginno, Y.W. Lim, P.L. Lott, I. Korf, F. Chédin, GC skew at the 5′ and 3′ ends of human genes links R-loop formation to epigenetic regulation and transcription termination, Genome Res. 23 (2013) 1590–1600. https://doi.org/10.1101/gr.158436.113.
[32] P.A. Ginno, P.L. Lott, H.C. Christensen, I. Korf, F. Chédin, R-loop formation is a distinctive characteristic of unmethylated human CpG island promoters, Mol. Cell. 45 (2012) 814–825. https://doi.org/10.1016/j.molcel.2012.01.017.
[33] Y. Sonobe, G. Ghadge, K. Masaki, A. Sendoel, E. Fuchs, R.P. Roos, Translation of dipeptide repeat proteins from the C9ORF72 expanded repeat is associated with cellular stress, Neurobiol. Dis. 116 (2018) 155–165. https://doi.org/10.1016/j.nbd.2018.05.009.
[34] R. Tabet, L. Schaeffer, F. Freyermuth, M. Jambeau, M. Workman, C.-Z. Lee, C.-C. Lin, J. Jiang, K. Jansen-West, H. Abou-Hamdan, L. Désaubry, T. Gendron, L. Petrucelli, F. Martin, C. Lagier-Tourenne, CUG initiation and frameshifting enable production of dipeptide repeat proteins from ALS/FTD C9ORF72 transcripts, Nat. Commun. 9 (2018) 1–14. https://doi.org/10.1038/s41467-017-02643-5.
[35] K.J. Trageser, C. Smith, F.J. Herman, K. Ono, G.M. Pasinetti, Mechanisms of Immune Activation by c9orf72-Expansions in Amyotrophic Lateral Sclerosis and Frontotemporal Dementia, Front. Neurosci. 13 (2019). https://doi.org/10.3389/fnins.2019.01298.
[36] Z. Xi, L. Zinman, D. Moreno, J. Schymick, Y. Liang, C. Sato, Y. Zheng, M. Ghani, S. Dib, J. Keith, J. Robertson, E. Rogaeva, Hypermethylation of the CpG island near the G4C2 repeat in ALS with a C9orf72 expansion, Am. J. Hum. Genet. 92 (2013) 981–989. https://doi.org/10.1016/j.ajhg.2013.04.017.
[37] P. Rizzu, C. Blauwendraat, S. Heetveld, E.M. Lynes, M. Castillo-Lizardo, A. Dhingra, E. Pyz, M. Hobert, M. Synofzik, J. Simón-Sánchez, M. Francescatto, P. Heutink, C9orf72 is differentially expressed in the central nervous system and myeloid cells and consistently reduced in C9orf72, MAPT and GRN mutation carriers, Acta Neuropathol. Commun. 4 (2016) 37. https://doi.org/10.1186/s40478-016-0306-7.
[38] M. Yang, C. Liang, K. Swaminathan, S. Herrlinger, F. Lai, R. Shiekhattar, J.-F. Chen, A C9ORF72/SMCR8-containing complex regulates ULK1 and plays a

dual role in autophagy, Sci. Adv. 2 (2016) e1601167. https://doi.org/10.1126/sciadv.1601167.
[39] M.E. Gurney, H. Pu, A.Y. Chiu, M.C. Dal Canto, C.Y. Polchow, D.D. Alexander, J. Caliendo, A. Hentati, Y.W. Kwon, H.X. Deng, Motor neuron degeneration in mice that express a human Cu,Zn superoxide dismutase mutation, Science. 264 (1994) 1772–1775. https://doi.org/10.1126/science.8209258.
[40] A. Atanasio, V. Decman, D. White, M. Ramos, B. Ikiz, H.-C. Lee, C.-J. Siao, S. Brydges, E. LaRosa, Y. Bai, W. Fury, P. Burfeind, R. Zamfirova, G. Warshaw, J. Orengo, A. Oyejide, M. Fralish, W. Auerbach, W. Poueymirou, J. Freudenberg, G. Gong, B. Zambrowicz, D. Valenzuela, G. Yancopoulos, A. Murphy, G. Thurston, K.-M.V. Lai, C9orf72 ablation causes immune dysregulation characterized by leukocyte expansion, autoantibody production, and glomerulonephropathy in mice, Sci. Rep. 6 (2016) 23204. https://doi.org/10.1038/srep23204.
[41] J. Chew, T.F. Gendron, M. Prudencio, H. Sasaguri, Y.-J. Zhang, M. Castanedes-Casey, C.W. Lee, K. Jansen-West, A. Kurti, M.E. Murray, K.F. Bieniek, P.O. Bauer, E.C. Whitelaw, L. Rousseau, J.N. Stankowski, C. Stetler, L.M. Daughrity, E.A. Perkerson, P. Desaro, A. Johnston, K. Overstreet, D. Edbauer, R. Rademakers, K.B. Boylan, D.W. Dickson, J.D. Fryer, L. Petrucelli, C9ORF72 repeat expansions in mice cause TDP-43 pathology, neuronal loss, and behavioral deficits, Science. 348 (2015) 1151–1154. https://doi.org/10.1126/science.aaa9344.
[42] J.G. O'Rourke, L. Bogdanik, A.K.M.G. Muhammad, T.F. Gendron, K.J. Kim, A. Austin, J. Cady, E.Y. Liu, J. Zarrow, S. Grant, R. Ho, S. Bell, S. Carmona, M. Simpkinson, D. Lall, K. Wu, L. Daughrity, D.W. Dickson, M.B. Harms, L. Petrucelli, E.B. Lee, C.M. Lutz, R.H. Baloh, C9orf72 BAC Transgenic Mice Display Typical Pathologic Features of ALS/FTD, Neuron. 88 (2015) 892–901. https://doi.org/10.1016/j.neuron.2015.10.027.
[43] Y. Liu, A. Pattamatta, T. Zu, T. Reid, O. Bardhi, D.R. Borchelt, A.T. Yachnis, L.P.W. Ranum, C9orf72 BAC Mouse Model with Motor Deficits and Neurodegenerative Features of ALS/FTD, Neuron. 90 (2016) 521–534. https://doi.org/10.1016/j.neuron.2016.04.005.
[44] B. Swinnen, A. Bento-Abreu, T.F. Gendron, S. Boeynaems, E. Bogaert, R. Nuyts, M. Timmers, W. Scheveneels, N. Hersmus, J. Wang, S. Mizielinska, A.M. Isaacs, L. Petrucelli, R. Lemmens, P. Van Damme, L. Van Den Bosch, W. Robberecht, A zebrafish model for C9orf72 ALS reveals RNA toxicity as a pathogenic mechanism, Acta Neuropathol. (Berl.). 135 (2018) 427–443. https://doi.org/10.1007/s00401-017-1796-5.
[45] X. Wang, L. Hao, T. Saur, K. Joyal, Y. Zhao, D. Zhai, J. Li, M. Pribadi, G. Coppola, B.M. Cohen, E.A. Buttner, Forward Genetic Screen in

Caenorhabditis elegans Suggests F57A10.2 and acp-4 As Suppressors of C9ORF72 Related Phenotypes, Front. Mol. Neurosci. 9 (2016) 113. https://doi.org/10.3389/fnmol.2016.00113.
[46] S. Almeida, E. Gascon, H. Tran, H.J. Chou, T.F. Gendron, S. Degroot, A.R. Tapper, C. Sellier, N. Charlet-Berguerand, A. Karydas, W.W. Seeley, A.L. Boxer, L. Petrucelli, B.L. Miller, F.-B. Gao, Modeling key pathological features of frontotemporal dementia with C9ORF72 repeat expansion in iPSC-derived human neurons, Acta Neuropathol. (Berl.). 126 (2013) 385–399. https://doi.org/10.1007/s00401-013-1149-y.
[47] R. Dafinca, J. Scaber, N. Ababneh, T. Lalic, G. Weir, H. Christian, J. Vowles, A.G.L. Douglas, A. Fletcher-Jones, C. Browne, M. Nakanishi, M.R. Turner, R. Wade-Martins, S.A. Cowley, K. Talbot, C9orf72 Hexanucleotide Expansions Are Associated with Altered Endoplasmic Reticulum Calcium Homeostasis and Stress Granule Formation in Induced Pluripotent Stem Cell-Derived Neurons from Patients with Amyotrophic Lateral Sclerosis and Frontotemporal Dementia, STEM CELLS. 34 (2016) 2063–2078. https://doi.org/10.1002/stem.2388.
[48] D. Sareen, J.G. O'Rourke, P. Meera, A.K.M.G. Muhammad, S. Grant, M. Simpkinson, S. Bell, S. Carmona, L. Ornelas, A. Sahabian, T. Gendron, L. Petrucelli, M. Baughn, J. Ravits, M.B. Harms, F. Rigo, C.F. Bennett, T.S. Otis, C.N. Svendsen, R.H. Baloh, Targeting RNA foci in iPSC-derived motor neurons from ALS patients with a C9ORF72 repeat expansion, Sci. Transl. Med. 5 (2013) 208ra149. https://doi.org/10.1126/scitranslmed.3007529.
[49] B.T. Selvaraj, M.R. Livesey, C. Zhao, J.M. Gregory, O.T. James, E.M. Cleary, A.K. Chouhan, A.B. Gane, E.M. Perkins, O. Dando, S.G. Lillico, Y.-B. Lee, A.L. Nishimura, U. Poreci, S. Thankamony, M. Pray, N.A. Vasistha, D. Magnani, S. Borooah, K. Burr, D. Story, A. McCampbell, C.E. Shaw, P.C. Kind, T.J. Aitman, C.B.A. Whitelaw, I. Wilmut, C. Smith, G.B. Miles, G.E. Hardingham, D.J.A. Wyllie, S. Chandran, C9ORF72 repeat expansion causes vulnerability of motor neurons to Ca 2+ -permeable AMPA receptor-mediated excitotoxicity, Nat. Commun. 9 (2018) 1–14. https://doi.org/10.1038/s41467-017-02729-0.
[50] B.T. Selvaraj, M.R. Livesey, S. Chandran, Modeling the C9ORF72 repeat expansion mutation using human induced pluripotent stem cells, Brain Pathol. Zurich Switz. 27 (2017) 518–524. https://doi.org/10.1111/bpa.12520.
[51] K. Takahashi, S. Yamanaka, Induction of pluripotent stem cells from mouse embryonic and adult fibroblast cultures by defined factors, Cell. 126 (2006) 663–676. https://doi.org/10.1016/j.cell.2006.07.024.
[52] Y. Maury, J. Côme, R.A. Piskorowski, N. Salah-Mohellibi, V. Chevaleyre, M. Peschanski, C. Martinat, S. Nedelec, Combinatorial analysis of

developmental cues efficiently converts human pluripotent stem cells into multiple neuronal subtypes, Nat. Biotechnol. 33 (2015) 89–96. https://doi.org/10.1038/nbt.3049.
[53] M.S. Rahman, N. Akhtar, H.M. Jamil, R.S. Banik, S.M. Asaduzzaman, TGF-β/BMP signaling and other molecular events: regulation of osteoblastogenesis and bone formation, Bone Res. 3 (2015) 1–20. https://doi.org/10.1038/boneres.2015.5.
[54] R.N. Wang, J. Green, Z. Wang, Y. Deng, M. Qiao, M. Peabody, Q. Zhang, J. Ye, Z. Yan, S. Denduluri, O. Idowu, M. Li, C. Shen, A. Hu, R.C. Haydon, R. Kang, J. Mok, M.J. Lee, H.L. Luu, L.L. Shi, Bone Morphogenetic Protein (BMP) signaling in development and human diseases, Genes Dis. 1 (2014) 87–105. https://doi.org/10.1016/j.gendis.2014.07.005.
[55] M.A. Lancaster, M. Renner, C.-A. Martin, D. Wenzel, L.S. Bicknell, M.E. Hurles, T. Homfray, J.M. Penninger, A.P. Jackson, J.A. Knoblich, Cerebral organoids model human brain development and microcephaly, Nature. 501 (2013) 373–379. https://doi.org/10.1038/nature12517.
[56] C. Lagier-Tourenne, M. Baughn, F. Rigo, S. Sun, P. Liu, H.-R. Li, J. Jiang, A.T. Watt, S. Chun, M. Katz, J. Qiu, Y. Sun, S.-C. Ling, Q. Zhu, M. Polymenidou, K. Drenner, J.W. Artates, M. McAlonis-Downes, S. Markmiller, K.R. Hutt, D.P. Pizzo, J. Cady, M.B. Harms, R.H. Baloh, S.R. Vandenberg, G.W. Yeo, X.-D. Fu, C.F. Bennett, D.W. Cleveland, J. Ravits, Targeted degradation of sense and antisense C9orf72 RNA foci as therapy for ALS and frontotemporal degeneration, Proc. Natl. Acad. Sci. U. S. A. 110 (2013) E4530-4539. https://doi.org/10.1073/pnas.1318835110.
[57] D. Bardelli, F. Sassone, C. Colombrita, C. Volpe, V. Gumina, S. Peverelli, I. Catusi, A. Ratti, V. Silani, P. Bossolasco, Reprogramming fibroblasts and peripheral blood cells from a C9ORF72 patient: A proof-of-principle study, J. Cell. Mol. Med. 24 (2020) 4051–4060. https://doi.org/10.1111/jcmm.15048.
[58] M.A. Lancaster, J.A. Knoblich, Generation of cerebral organoids from human pluripotent stem cells, Nat. Protoc. 9 (2014) 2329–2340. https://doi.org/10.1038/nprot.2014.158.
[59] J. Nichols, B. Zevnik, K. Anastassiadis, H. Niwa, D. Klewe-Nebenius, I. Chambers, H. Schöler, A. Smith, Formation of Pluripotent Stem Cells in the Mammalian Embryo Depends on the POU Transcription Factor Oct4, Cell. 95 (1998) 379–391. https://doi.org/10.1016/S0092-8674(00)81769-9.
[60] M.A. Farg, A. Konopka, K.Y. Soo, D. Ito, J.D. Atkin, The DNA damage response (DDR) is induced by the C9orf72 repeat expansion in amyotrophic lateral sclerosis, Hum. Mol. Genet. 26 (2017) 2882–2896. https://doi.org/10.1093/hmg/ddx170.

[61] R.I. Yarden, S. Pardo-Reoyo, M. Sgagias, K.H. Cowan, L.C. Brody, BRCA1 regulates the G2/M checkpoint by activating Chk1 kinase upon DNA damage, Nat. Genet. 30 (2002) 285–289. https://doi.org/10.1038/ng837.
[62] T.T. Paull, E.P. Rogakou, V. Yamazaki, C.U. Kirchgessner, M. Gellert, W.M. Bonner, A critical role for histone H2AX in recruitment of repair factors to nuclear foci after DNA damage, Curr. Biol. CB. 10 (2000) 886–895. https://doi.org/10.1016/s0960-9822(00)00610-2.
[63] S. Corrà, R. Salvadori, L. Bee, V. Barbieri, M. Mognato, Analysis of DNA-damage response to ionizing radiation in serum-shock synchronized human fibroblasts, Cell Biol. Toxicol. 33 (2017) 373–388. https://doi.org/10.1007/s10565-017-9394-9.
[64] D.K. Alves-Fernandes, M.G. Jasiulionis, The Role of SIRT1 on DNA Damage Response and Epigenetic Alterations in Cancer, Int. J. Mol. Sci. 20 (2019). https://doi.org/10.3390/ijms20133153.
[65] M. Niblock, B.N. Smith, Y.-B. Lee, V. Sardone, S. Topp, C. Troakes, S. Al-Sarraj, C.S. Leblond, P.A. Dion, G.A. Rouleau, C.E. Shaw, J.-M. Gallo, Retention of hexanucleotide repeat-containing intron in C9orf72 mRNA: implications for the pathogenesis of ALS/FTD, Acta Neuropathol. Commun. 4 (2016). https://doi.org/10.1186/s40478-016-0289-4.
[66] S. Ciura, S. Lattante, I. Le Ber, M. Latouche, H. Tostivint, A. Brice, E. Kabashi, Loss of function of C9orf72 causes motor deficits in a zebrafish model of amyotrophic lateral sclerosis, Ann. Neurol. 74 (2013) 180–187. https://doi.org/10.1002/ana.23946.
[67] R. Lopez-Gonzalez, Y. Lu, T.F. Gendron, A. Karydas, H. Tran, D. Yang, L. Petrucelli, B.L. Miller, S. Almeida, F.-B. Gao, Poly(GR) in C9ORF72-Related ALS/FTD Compromises Mitochondrial Function and Increases Oxidative Stress and DNA Damage in iPSC-Derived Motor Neurons, Neuron. 92 (2016) 383–391. https://doi.org/10.1016/j.neuron.2016.09.015.
[68] C.J. Donnelly, P.-W. Zhang, J.T. Pham, A.R. Haeusler, A.R. Heusler, N.A. Mistry, S. Vidensky, E.L. Daley, E.M. Poth, B. Hoover, D.M. Fines, N. Maragakis, P.J. Tienari, L. Petrucelli, B.J. Traynor, J. Wang, F. Rigo, C.F. Bennett, S. Blackshaw, R. Sattler, J.D. Rothstein, RNA toxicity from the ALS/FTD C9ORF72 expansion is mitigated by antisense intervention, Neuron. 80 (2013) 415–428. https://doi.org/10.1016/j.neuron.2013.10.015.
[69] J.-H. Lee, T.T. Paull, Activation and regulation of ATM kinase activity in response to DNA double-strand breaks, Oncogene. 26 (2007) 7741–7748. https://doi.org/10.1038/sj.onc.1210872.
[70] J. Wu, M.S.Y. Huen, L.-Y. Lu, L. Ye, Y. Dou, M. Ljungman, J. Chen, X. Yu, Histone Ubiquitination Associates with BRCA1-Dependent DNA Damage

Response, Mol. Cell. Biol. 29 (2009) 849–860. https://doi.org/10.1128/MCB.01302-08.
[71] A.R. Haeusler, C.J. Donnelly, G. Periz, E.A.J. Simko, P.G. Shaw, M.-S. Kim, N.J. Maragakis, J.C. Troncoso, A. Pandey, R. Sattler, J.D. Rothstein, J. Wang, C9orf72 nucleotide repeat structures initiate molecular cascades of disease, Nature. 507 (2014) 195–200. https://doi.org/10.1038/nature13124.
[72] K. Reddy, M.H.M. Schmidt, J.M. Geist, N.P. Thakkar, G.B. Panigrahi, Y.-H. Wang, C.E. Pearson, Processing of double-R-loops in (CAG)·(CTG) and C9orf72 (GGGGCC)·(GGCCCC) repeats causes instability, Nucleic Acids Res. 42 (2014) 10473–10487. https://doi.org/10.1093/nar/gku658.
[73] J. Jiang, Q. Zhu, T.F. Gendron, S. Saberi, M. McAlonis-Downes, A. Seelman, J.E. Stauffer, P. Jafar-nejad, K. Drenner, D. Schulte, S. Chun, S. Sun, S.-C. Ling, B. Myers, J. Engelhardt, M. Katz, M. Baughn, O. Platoshyn, M. Marsala, A. Watt, C.J. Heyser, M.C. Ard, L. De Muynck, L.M. Daughrity, D.A. Swing, L. Tessarollo, C.J. Jung, A. Delpoux, D.T. Utzschneider, S.M. Hedrick, P.J. de Jong, D. Edbauer, P. Van Damme, L. Petrucelli, C.E. Shaw, C.F. Bennett, S. Da Cruz, J. Ravits, F. Rigo, D.W. Cleveland, C. Lagier-Tourenne, Gain of toxicity from ALS/FTD-linked repeat expansions in C9ORF72 is alleviated by antisense oligonucleotides targeting GGGGCC-containing RNAs, Neuron. 90 (2016) 535–550. https://doi.org/10.1016/j.neuron.2016.04.006.
[74] H. Wagner, S. Bauer, All is not Toll: new pathways in DNA recognition, J. Exp. Med. 203 (2006) 265–268. https://doi.org/10.1084/jem.20052191.
[75] D. Diao, H. Wang, T. Li, Z. Shi, X. Jin, T. Sperka, X. Zhu, M. Zhang, F. Yang, Y. Cong, L. Shen, Q. Zhan, J. Yan, Z. Song, Z. Ju, Telomeric epigenetic response mediated by Gadd45a regulates stem cell aging and lifespan, EMBO Rep. 19 (2018). https://doi.org/10.15252/embr.201745494.
[76] D.W. Dickson, M.C. Baker, J.L. Jackson, M. DeJesus-Hernandez, N.A. Finch, S. Tian, M.G. Heckman, C. Pottier, T.F. Gendron, M.E. Murray, Y. Ren, J.S. Reddy, N.R. Graff-Radford, B.F. Boeve, R.C. Petersen, D.S. Knopman, K.A. Josephs, L. Petrucelli, B. Oskarsson, J.W. Sheppard, Y.W. Asmann, R. Rademakers, M. van Blitterswijk, Extensive transcriptomic study emphasizes importance of vesicular transport in C9orf72 expansion carriers, Acta Neuropathol. Commun. 7 (2019) 150. https://doi.org/10.1186/s40478-019-0797-0.
[77] E.Y. Liu, J. Russ, E.B. Lee, Neuronal Transcriptome from C9orf72 Repeat Expanded Human Tissue is Associated with Loss of C9orf72 Function, Free Neuropathol. 1 (2020). https://www.ncbi.nlm.nih.gov/pmc/articles/PMC7470232/ (accessed December 6, 2020).

[78] F.A. Sultan, J.D. Sweatt, The role of the Gadd45 family in the nervous system: a focus on neurodevelopment, neuronal injury, and cognitive neuroepigenetics, Adv. Exp. Med. Biol. 793 (2013) 81–119. https://doi.org/10.1007/978-1-4614-8289-5_6.
[79] P. Baskaran, C. Shaw, S. Guthrie, TDP-43 causes neurotoxicity and cytoskeletal dysfunction in primary cortical neurons, PloS One. 13 (2018) e0196528. https://doi.org/10.1371/journal.pone.0196528.
[80] J. Eira, C.S. Silva, M.M. Sousa, M.A. Liz, The cytoskeleton as a novel therapeutic target for old neurodegenerative disorders, Prog. Neurobiol. 141 (2016) 61–82. https://doi.org/10.1016/j.pneurobio.2016.04.007.
[81] T. Leiva-Rodríguez, D. Romeo-Guitart, S. Marmolejo-Martínez-Artesero, M. Herrando-Grabulosa, A. Bosch, J. Forés, C. Casas, ATG5 overexpression is neuroprotective and attenuates cytoskeletal and vesicle-trafficking alterations in axotomized motoneurons, Cell Death Dis. 9 (2018) 626. https://doi.org/10.1038/s41419-018-0682-y.
[82] M.S. Lyon, M. Wosiski-Kuhn, R. Gillespie, J. Caress, C. Milligan, Inflammation, Immunity, and amyotrophic lateral sclerosis: I. Etiology and pathology, Muscle Nerve. 59 (2019) 10–22. https://doi.org/10.1002/mus.26289.
[83] P.A. McCombe, R.D. Henderson, The Role of Immune and Inflammatory Mechanisms in ALS, Curr. Mol. Med. 11 (2011) 246–254. https://doi.org/10.2174/156652411795243450.
[84] J.H. Hor, E.S.-Y. Soh, L.Y. Tan, V.J.W. Lim, M.M. Santosa, Winanto, B.X. Ho, Y. Fan, B.-S. Soh, S.-Y. Ng, Cell cycle inhibitors protect motor neurons in an organoid model of Spinal Muscular Atrophy, Cell Death Dis. 9 (2018) 1–12. https://doi.org/10.1038/s41419-018-1081-0.
[85] I.I. Kruman, R.P. Wersto, F. Cardozo-Pelaez, L. Smilenov, S.L. Chan, F.J. Chrest, R. Emokpae, M. Gorospe, M.P. Mattson, Cell Cycle Activation Linked to Neuronal Cell Death Initiated by DNA Damage, Neuron. 41 (2004) 549–561. https://doi.org/10.1016/S0896-6273(04)00017-0.
[86] H.J. Rideout, Q. Wang, D.S. Park, L. Stefanis, Cyclin-Dependent Kinase Activity Is Required for Apoptotic Death But Not Inclusion Formation in Cortical Neurons after Proteasomal Inhibition, J. Neurosci. 23 (2003) 1237–1245. https://doi.org/10.1523/JNEUROSCI.23-04-01237.2003.
[87] B.-Q. Lai, B. Feng, M.-T. Che, L.-J. Wang, S. Cai, M.-Y. Huang, H.-Y. Gu, B. Jiang, E.-A. Ling, M. Li, X. Zeng, Y.-S. Zeng, A Modular Assembly of Spinal Cord-Like Tissue Allows Targeted Tissue Repair in the Transected Spinal Cord, Adv. Sci. 5 (2018) 1800261. https://doi.org/10.1002/advs.201800261.
[88] J. Jo, Y. Xiao, A.X. Sun, E. Cukuroglu, H.-D. Tran, J. Göke, Z.Y. Tan, T.Y. Saw, C.-P. Tan, H. Lokman, Y. Lee, D. Kim, H.S. Ko, S.-O. Kim, J.H. Park, N.-J. Cho, T.M. Hyde, J.E. Kleinman, J.H. Shin, D.R. Weinberger, E.K. Tan, H.S. Je, H.-H.

Ng, Midbrain-like Organoids from Human Pluripotent Stem Cells Contain Functional Dopaminergic and Neuromelanin-Producing Neurons, Cell Stem Cell. 19 (2016) 248–257. https://doi.org/10.1016/j.stem.2016.07.005.
[89] G. Quadrato, T. Nguyen, E.Z. Macosko, J.L. Sherwood, S. Min Yang, D.R. Berger, N. Maria, J. Scholvin, M. Goldman, J.P. Kinney, E.S. Boyden, J.W. Lichtman, Z.M. Williams, S.A. McCarroll, P. Arlotta, Cell diversity and network dynamics in photosensitive human brain organoids, Nature. 545 (2017) 48–53. https://doi.org/10.1038/nature22047.
[90] S. Herranz-Martin, J. Chandran, K. Lewis, P. Mulcahy, A. Higginbottom, C. Walker, I.M.-P. y Valenzuela, R.A. Jones, I. Coldicott, T. Iannitti, M. Akaaboune, S.F. El-Khamisy, T.H. Gillingwater, P.J. Shaw, M. Azzouz, Viral delivery of C9orf72 hexanucleotide repeat expansions in mice leads to repeat-length-dependent neuropathology and behavioural deficits, Dis. Model. Mech. 10 (2017) 859–868. https://doi.org/10.1242/dmm.029892.
[91] B.T. Selvaraj, M.R. Livesey, C. Zhao, J.M. Gregory, O.T. James, E.M. Cleary, A.K. Chouhan, A.B. Gane, E.M. Perkins, O. Dando, S.G. Lillico, Y.-B. Lee, A.L. Nishimura, U. Poreci, S. Thankamony, M. Pray, N.A. Vasistha, D. Magnani, S. Borooah, K. Burr, D. Story, A. McCampbell, C.E. Shaw, P.C. Kind, T.J. Aitman, C.B.A. Whitelaw, I. Wilmut, C. Smith, G.B. Miles, G.E. Hardingham, D.J.A. Wyllie, S. Chandran, C9ORF72 repeat expansion causes vulnerability of motor neurons to Ca2+-permeable AMPA receptor-mediated excitotoxicity, Nat. Commun. 9 (2018) 347. https://doi.org/10.1038/s41467-017-02729-0.
[92] K. Zhang, C.J. Donnelly, A.R. Haeusler, J.C. Grima, J.B. Machamer, P. Steinwald, E.L. Daley, S.J. Miller, K.M. Cunningham, S. Vidensky, S. Gupta, M.A. Thomas, I. Hong, S.-L. Chiu, R.L. Huganir, L.W. Ostrow, M.J. Matunis, J. Wang, R. Sattler, T.E. Lloyd, J.D. Rothstein, The C9orf72 repeat expansion disrupts nucleocytoplasmic transport, Nature. 525 (2015) 56–61. https://doi.org/10.1038/nature14973.
[93] S.Y. Choi, R. Lopez-Gonzalez, G. Krishnan, H.L. Phillips, A.N. Li, W.W. Seeley, W.-D. Yao, S. Almeida, F.-B. Gao, C9ORF72-ALS/FTD-associated poly(GR) binds Atp5a1 and compromises mitochondrial function in vivo, Nat. Neurosci. 22 (2019) 851–862. https://doi.org/10.1038/s41593-019-0397-0.
[94] J. Mata-Garrido, O. Tapia, I. Casafont, M.T. Berciano, A. Cuadrado, M. Lafarga, Persistent accumulation of unrepaired DNA damage in rat cortical neurons: nuclear organization and ChIP-seq analysis of damaged DNA, Acta Neuropathol. Commun. 6 (2018) 68. https://doi.org/10.1186/s40478-018-0573-6.

SCIENTIFIC PRODUCTION.

Taiana Michela, Biella Fabio, Margherita Bersani, Nizzardo Monica, Corti Stefania - “Morpholino treatment in iPSC-derived Motor Neuron alters C9orf72 Pathological Hallmarks - Manuscript in Preparation

D. Gagliardi, G. Costamagna, M. Taiana, L. Andreoli, F. Biella, M. Bersani, N. Bresolin, G.P. Comi, S. Corti. “Insights into disease mechanisms and potential therapeutics for C9orf72-related amyotrophic lateral sclerosis/frontotemporal dementia” Ageing Research Reviews. 2020 Sep 21:101172. PMID: 32971256, doi: 10.1016/j.arr.2020.101172. Online ahead of print. - Review

Roberta De Gioia*****, Fabio Biella*****, Gaia Citterio, Federica Rizzo, Elena Abati, Monica Nizzardo, Nereo Bresolin, Giacomo Pietro Comi, Stefania Corti. “Neural Stem Cell Transplantation for Neurodegenerative Diseases”. Int. J. of Mol. Sci., 21 (9), E3103, April 28, 2020 PMID: 32354178, doi: 10.3390/ijms21093103. – Review **(*Co-first author)**

Giacomo Bitetto, Maria Chiara Malaguti ,Roberto Ceravolo, Edoardo Monfrini, Letizia Straniero, Alberto Morini, Raffaella Di Giacopo, Daniela Frosini, Giovanni Palermo, Fabio Biella, Dario Ronchi, Stefano Duga, Franco Taroni, Stefania Corti, Giacomo P Comi, Nereo

Bresolin, Bruno Giometto, Alessio Di Fonzo. “SLC25A46 Mutations in Patients With Parkinson's Disease and Optic Atrophy”. Parkinsonism Relat Disord, 74, 1-5, April 02, 2020 PMID: 32259769, doi: 10.1016/j.parkreldis.2020.03.018. – Research Article

Lenzken S. C., Levone B. R., Filosa G., Antonaci M., Conte F., Kızılırmak Ç., Reber S., Loffreda A., Biella F., Ronchi A. E., Mühlemann O., Bachi A., Ruepp M.-D., Barabino S. M. L., 2019 – “FUS-dependent phase separation initiates double-strand break repair”. bioRxiv 798884; doi: 10.1101/798884 - Pre-printed Article

Biella F., Taiana M., Bersani M., Nizzardo M., Rizzuti M., Levone BR., Bresolin N., Comi G.P., Barabino S., Corti S., 2019 – “Investigation of molecular pathological hallmarks and therapeutic strategies in C9ORF72 human lines”. ENCALS 2019, Tours, France – Conference Poster

Lenzken S. C., Antonaci M., Levone B. R., Conte F., Kızılırmak Ç., Biella F., Filosa G., Ruepp M.-D., Barabino S. M. L., 2019 – “Role of Fused in Sarcoma/Translocated in Liposarcoma (FUS/TLS) in Genome Maintenance and DNA Damage Response”. Swiss RNA Workshop, Basel, Switzerland. – Conference Abstract

ACKNOWLEDGMENTS.

I wish to thank professor Stefania Corti for the opportunity to join her laboratory during my PhD project.

I wish to thank Dr. Michela Taiana and Dr. Monica Nizzardo for the support and the patient mostly while supervising my thesis work.

A thanks to my laboratory colleagues Dr. Mafalda Rizzuti, Dr. Federica Rizzo, Dr. Valentina Melzi and Dr. Dario Ronchi for sharing the work we've done, Dr. Sabrina Lucchiari and Dr. Serena Pagliarani for welcoming me when I joined the lab and Dr. Sabrina Salani for the kindness and teaching me how to work with iPSCs.

A very big thanks to the FantaLab and its wonderful people Dr. Margherita Bersani, Dr. Noemi Galli, Dr. Elisa Pagliari, Dr. Stefano Ghezzi, Dr. Nicolò Alerni, Dr. Roberta De Gioia and Dr. Giovanna Gaburri. I couldn't have made it without your friendship and support.

I'm very thankful to the people of my master thesis lab, professor Silvia Barabino and Dr. Silvia Carolina Lenzken for what they taught me, to Dr. Alessio Di Fonzo and the people of his lab Dr. Ilaria Trezzi, Dr. Mattia Tosi, Dr. Manuela Magni, Dr. Edoardo Monfrini, Dr. Giacomo Bitetto, Dr.Giulia Lazzeri, Dr.Maria Vizziello, Dr. Emanuele Frattini, Dr. Federica Arienti, Dr. Arianna Manini and Dr. Marco Precetti for the support and the critical discussions we had.

And I'm thankful to the people I met in various moment which have been friendly and supportive. Dr. Francesca Conte, Dr. Çise Kızılırmak, Dr. Annalisa Anzani, Dr. Marco Antonaci, Dr. Mirella Parrella, Dr. Clara Volpe, Dr. Donatella Bardelli, Dr. Annalisa Anzani

E soprattutto vorrei ringraziare la mia famiglia per l'affetto ed il supporto, mia madre Candida Caiani, mio padre Lorenzo Biella, mio fratello Dr.Marco Biella, mio zio Pietro Caiani e mia zia Gina Torrini.